12-2001

Teleoperability and dynamic teleoperability

Pamela Gail Murray

To the Graduate Council:

I am submitting herewith a thesis written by Pamela Gail Murray entitled "Teleoperability and dynamic teleoperability." I have examined the final electronic copy of this thesis for form and content and recommend that it be accepted in partial fulfillment of the requirements for the degree of Master of Science, with a major in Mechanical Engineering.

Reid L. Kress, Major Professor

We have read this thesis and recommend its acceptance:

William R. Hamel, Gary V. Smith, Tyler A. Kress

Accepted for the Council:
Carolyn R. Hodges

Vice Provost and Dean of the Graduate School

(Original signatures are on file with official student records.)

To the Graduate Council:

I am submitting herewith a thesis written by Pamela Gail Murray entitled "Teleoperability and Dynamic Teleoperability." I have examined the final paper copy of this thesis for form and content and recommend that it be accepted in partial fulfillment of the requirements for the degree of Master of Science, with a major in Mechanical Engineering.

Reid Kress

Reid L. Kress, Major Professor

We have read this thesis
and recommend its acceptance:

William R. Hamel

William R. Hamel

Gary V. Smith

Gary V. Smith

Tyler Kress

Tyler A. Kress

Accepted for the Council:

Vice Provost and
Dean of Graduate Studies

TELEOPERABILITY AND DYNAMIC TELEOPERABILITY

A Thesis
Presented for the
Master of Science
Degree
The University of Tennessee, Knoxville

Pamela Gail Murray
December 2001

ACKNOWLEDGMENTS

I would first like to thank Dr. Reid Kress for allowing me to work with him on his teleoperability research. I would also like to thank my committee: Dr. Bill Hamel, Dr. Gary Smith, and Dr. Tyler Kress for their suggestions. I would also like to thank Dr. Bill Hamel for my graduate research assistantship. Thanks also to former Mechanical and Aerospace Engineering and Engineering Science (MAES) department head Dr. Don Dareing for his help in securing funding for my graduate education and for his support of my endeavors. I would also like to acknowledge the financial support provided by the Graduate School and the MAES Department.

I would also like to thank my former advisors and their groups: Dr. Dana Yoerger and the Deep Submergence Laboratory at Woods Hole Oceanographic Institution and Dr. Lynne Parker and the Center for Engineering Science and Advanced Research at Oak Ridge National Laboratory for the challenging learning experiences I had and for the mentoring I continue to receive.

I also sincerely thank my parents Bill and Patricia Murray for their continued love, support, and guidance.

ABSTRACT

Teleoperated systems are used in many hostile environments and are therefore very complex. Current design procedures select kinematic configurations based on the designer's past experience and some standard practice guidelines. Yet, no unifying theory exists to quantifiably discern between competing kinematic designs and guide in the selection of key operational strategies such as indexing, length scaling, and mass scaling. Manipulability and dynamic manipulability theory attempt to present a quantitative measure which can be used to evaluate a robotic manipulator. This thesis expands this theory to teleoperability and dynamic teleoperability which can be used to evaluate teleoperated manipulator systems.

The mathematical developments of teleoperability and dynamic teleoperability are presented. The behavior of the teleoperability and dynamic teleoperability measures in various operational conditions is presented. Special attention is given to the effects of indexing, length scaling, and mass scaling between the master and slave. Simple experimental results validate the theory.

Teleoperability, dynamic teleoperability and the associated ellipsoids and measures are useful concepts for the design, implementation, and selection of teleoperated systems. Specifically, this theory can be used in the selection of master and slave configurations, guide in control system design, and provide insight into necessary and/or helpful operational features for teleoperated and telerobotic systems.

TABLE OF CONTENTS

CHAPTER PAGE

LIST OF FIGURES

FIGURE PAGE

NOMENCLATURE

Symbol	Representation	[units] in terms of length [L], mass [m], and time [t]
a	Fitts' human linkage constant	[t]
b	Fitts' human linkage constant	[t]
d	movement distance	[L]
DTO_M	dynamic teleoperability measure	[-]
$\mathbf{f}$	end-effector force (mx1)	$\left[\frac{mL}{t^2}\right]$
$\mathbf{F}_{ENV}$	force from end-effector at slave end (mx1)	$\left[\frac{mL}{t^2}\right]$
$\mathbf{F}_H$	hand force (mx1)	$\left[\frac{mL}{t^2}\right]$
$\mathbf{g}$	gravitational forces (nx1)	$\left[\frac{mL^2}{t^2}\right]$
$\mathbf{h}$	centrifugal and Coriolis forces (nx1)	$\left[\frac{mL^2}{t^2}\right]$
ID	index of difficulty	[-]
$\mathbf{J}$	Jacobian (mxn)	[-, L, or 1/L]
$\dot{\mathbf{J}}$	derivative of Jacobian (mxn)	[1/t, L/t, , 1/Lt]
$\mathbf{J}_{DTO}$	dynamic teleoperability Jacobian (mxm)	[-, L, L^2, 1/L, $1/L^2$]
$\mathbf{J}_{TO}$	teleoperability Jacobian (mxm)	[-, L, L^2, 1/L, $1/L^2$]
$\mathbf{J}_R$	rotational component of Jacobian (3xn)	[-, 1/L]

$\mathbf{J}_T$	translational component of Jacobian (3xn)	[-, L]
l_{c_i}	length to center of mass of link i	[L]
l_i	length of link i	[L]
m_i	mass of link i	[m]
$\mathbf{M}$	inertia matrix (nxn)	$\left[mL^2\right]$
MT	movement time	[t]
N	rank of $\mathbf{J}_T$	[-]
$\mathbf{q}$	joint position (nx1)	[-]
$\dot{\mathbf{q}}$	joint velocity (nx1)	[1/t]
$\ddot{\mathbf{q}}$	joint acceleration (nx1)	$\left[\frac{1}{t^2}\right]$
TO_M	teleoperability measure	[-]
$\mathbf{v}$	end-effector velocity (mx1)	[l/t]
$\dot{\mathbf{v}}$	end-effector acceleration (mx1)	$\left[\frac{l}{t^2}\right]$
$\tilde{\dot{\mathbf{v}}}$	modified end-effector acceleration (mx1)	$\left[\frac{l}{t^2}\right]$
w	target diameter	[L]
β	length scaling factor	[-]
δ	force reflection scaling factor	[-]
γ	mass scaling factor	[-]
θ	joint angle	[-]

τ	joint torque (nx1)	$\left[\frac{mL^2}{t^2}\right]$
$\tilde{\tau}$	modified joint torque (nx1)	$\left[\frac{mL^2}{t^2}\right]$

Note: Subscripts *m* and *s* denote variables for the master and slave, respectively.

1 Introduction

According to Raimondi [1988], "The telemanipulator is a device which allows an operator to perform a task at a distance, in a hostile environment where human access is impossible or inadvisable." Common hostile environments include outer space, the deep sea, and radioactive areas. Research at Oak Ridge National Laboratory and The University of Tennessee focuses on telemanipulators for use in radioactive environments such as hot cells and process canyons encountered during nuclear research, weapons production, and nuclear power generation. The severe health hazards associated with a radioactive environment override cost concerns associated with telerobotic systems. A telemanipulator or teleoperator system is actually composed of two manipulators -- a master manipulator that is held by a human operator and a slave manipulator that will perform (or try to perform) the desired task. The master manipulator is located in a safe, clean environment where information (typically visual, sound, and force information) is fed back from the slave manipulator to the human operator. The slave manipulator is located at the intended task typically at some distance from the human operator.

A telerobot is a teleoperated system with added autonomous capabilities or a robot controlled by a human supervisory operator who has various levels of intervention capability. Vertut [1985] defines an ideal telerobot as a system providing maximum autonomy and versatility. Robotic systems like CNC machines provide significant autonomy but little versatility while teleoperated systems like hand tools provide more versatility with less autonomy. Therefore, there are two paths to the ideal telerobot.

In the late 1940s, Goertz and his colleagues at Argonne National Laboratory developed one of the earliest recognizable mechanical master/slave manipulators and later refined its force-reflecting capabilities **[Goertz, 52]**. Force reflection refers to the capability of reflecting the external forces experienced by the slave manipulator to the master manipulator and is typically described as bilateral control: force on the slave (master) will cause the master (slave) to move. In the early 1950s, Goertz and his colleagues developed an electric master/slave manipulator in which each slave joint servo was tied directly to the master joint servo, and both the master and slave manipulators were kinematically similar **[Goertz, 54]**. Carl Flateau **[1965]** made major contributions to teleoperator development in the 1960s introducing position-force type control. Hydraulics, too, have been used from almost the beginning of this field starting with the Handyman system developed by Mosher and his team at General Electric in the late 1950s **[Johnsen, 67]**. Today, hydraulic actuators are not usually selected for high radiation environments because the hydraulic fluid and its associated seals suffer from radiation-induced degradation, but some examples of high radiation applications have been found **[Kaye, 92]** and **[Rule, 98]**. Interested readers can refer to Vertut **[1985]** for a more detailed discussion of the history of teleoperator systems.

Many challenges exist during the design of teleoperated systems. The designer must determine the optimal master and slave kinematics. The kinematic design includes the determination of the number of degrees of freedom (DOF), the need for redundancy, and whether to use a similar or dissimilar system. In addition, the size of the system must be determined. The length, cross-section, and mass of the links must be chosen. Generally, mass is minimized, but the impact of this minimization must be evaluated. These choices dictate motor sizes. The control scheme for the teleoperated system must also be designed at the servo-level and operator level. At the operator level, this includes providing for obstacle and singularity avoidance as well as reducing redundancy in redundant arms. The designer must also design an intuitive human machine interface.

Oak Ridge National Laboratory has developed a series of teleoperated and telerobotic manipulator systems over the past quarter century. These manipulator systems include similar master/slave systems with joint-to-joint controllers, dissimilar master/slave systems, electrical systems, hydraulic systems, large long-reach telerobotic systems, and mobile teleoperated platforms. Many of these systems are described in detail in Kress [1997]. When each of these systems was designed and constructed, there was no simple unifying theory to quantifiably discern between competing kinematic designs and/or to guide in the selection of key operational strategies such as indexing. Many of the design tradeoffs generally associated with these issues were typically settled based on the experience of the teleoperated system designer. Therefore, measures that could be used to numerically evaluate design alternatives would be of great benefit to the designer.

The goal of this thesis is to present the theory of teleoperability and dynamic teleoperability and to suggest that it be used as a simple method to numerically compare alternate kinematic configurations and operational and control strategies for teleoperated and telerobotic manipulator systems. Specifically, it will be shown that the developed teleoperability measure can be used in kinematic design and that the dynamic teleoperability measure can be used in sizing the teleoperated system. In addition, both measures will be useful in selecting manipulators and in determining optimal control strategies. A second goal is to attempt to mathematically explain some of the basic behaviors observed in operating teleoperated and telerobotic manipulator systems in some simple example scenarios. Two and three DOF systems are used during the development of the teleoperability and dynamic teleoperability concepts. Clearly, future work must extend this development to systems with more DOF.

The chapters of this thesis are divided as follows. The second chapter presents the conceptual development of teleoperability and dynamic teleoperability theory from previous work. The third chapter covers the mathematical development of teleoperability and dynamic teleoperability and their respective ellipsoids and measures. The fourth chapter states the implications of teleoperability and dynamic teleoperability for various general teleoperator and telerobot configurations and control strategies. The fifth chapter contains results of the calculation of the teleoperability and dynamic teleoperability measure for simplified master/slave systems under different conditions. The sixth chapter presents experimental results that verify the teleoperability and dynamic teleoperability theory. The seventh chapter contains a discussion of teleoperability in the context of teleoperated manipulator system design. Finally, the eighth chapter offers the conclusions of this research.

2 Conceptual Background

Teleoperability and the associated concept of dynamic teleoperability are presented as the latest extension of manipulability which was first introduced in the 1980s by Tsuneo Yoshikawa **[1985a]**. Conceptually, manipulability looks at how an "n-sphere" (2 DOF: n-sphere = circle, 3 DOF: n-sphere = sphere, 4 DOF: n-sphere = 4-sphere) in joint velocity space is mapped to end-effector space. A spherical space gives uniform performance throughout the workspace. Issues of concern include:

1) Will the joint-space velocity sphere maintain a spherical shape in end-effector space or will it become elliptical?

2) If it becomes elliptical, then will it degenerate and lose a dimension?

3) How will the joint space velocity sphere scale?

4) How do changes in manipulator kinematics affect the relationship between the joint space velocity sphere and the end-effector velocity sphere?

The manipulability measure presented one of the first quantitative measures for evaluating a manipulator's ability to position and orient its end-effector. This measure can now be used in optimal design and control of manipulators. For example, in redundancy resolution, an arm configuration can be selected using the manipulability measure as a performance criterion. Since this foundational work, the concept of manipulability has been further developed and applied. The rest of this section presents the significant developments in manipulability theory that have led to the development of teleoperability and dynamic teleoperability.

Before the concept of manipulability had been introduced, Salisbury and Craig **[1982]** described methods of analyzing kinematic factors. The application presented is that of an articulated, multi-fingered hand. Kinematic analysis is approached from the viewpoint of mobility which they define as "the number of independent parameters necessary to specify completely the position of every body in the system at an instant" and connectivity which is defined as determining the mobility of "subchains connecting two bodies in question". This paper also examines methods of quantifying workspace quality including error and noise propagation. In the study of noise propagation, $\mathbf{J}\mathbf{J}^T$ where $\mathbf{J}$ is the Jacobian is first used as a measure. Manipulability, too, relies on this measure. In their optimization of hand kinematic parameters, "potential designs are scored on the basis of working volume, defined as the volume within which the object may be positioned given a fixed grasp." The manipulability measure used by Yoshikawa is proportional to the working volume of the end-effector.

In 1984, Yoshikawa **[1984]** first presented the manipulability (here called the manipulatability) measure for an arm posture and described the manipulability concept. It is introduced in the context of evaluating redundant manipulator configurations but can also be applied to non-redundant manipulators. Based on this measure, control algorithms are presented to avoid singularities or obstacles. The basis for the control algorithm is to attempt to execute the desired task and if multiple solutions exist evaluate these using the manipulability measure as a performance criterion.

Other measures were also introduced to measure the manipulability of redundant manipulators. Klein **[1985]** discusses how redundancy in manipulators can be used to avoid obstacles and keep the arm in what he termed "dexterous" configurations. Several measures of manipulability including Yoshikawa's measure, the determinant, and condition number are compared. The minimum singular value is offered as an alternative based on the fact that the "determinant and condition number differ only by factors of the minimum singular value" and the "minimum singular value typically determines singularities."

In 1985, Yoshikawa discussed properties of his previously proposed manipulability measure **[Yoshikawa, 85a]**. Several manipulators are studied to determine their optimal postures based on the manipulability measure. An interesting conclusion is that the human arm taken as a two-link manipulator is typically used in the optimal configuration from a manipulability viewpoint. For a two-link manipulator with equal link lengths, the manipulability measure is at a maximum when the "elbow" angle is ninety degrees, and this is the standard arm configuration for many human tasks. Similarly, the finger when used to handle small objects is used in the optimal configuration of a four-joint robotic finger. A property presented is that when the maximum velocities of all the joints are not the same, they should be normalized. This normalization does not change the relative shape of the manipulability measure. A mention is also made of a competing measure introduced by Salisbury and Craig in "Articulated hands: Force control and kinematic issues" and the difference in what they measure. The resulting difference in optimal postures of a simple mechanism is also presented.

Yoshikawa went on to introduce the concept of the dynamic manipulability measure and ellipsoid as an extension of his earlier manipulability measure and ellipsoid **[Yoshikawa 85b, 90]**. Basic properties are presented. A simple two-link mechanism is then analyzed with the new measure. The measure is presented both with and without gravity effects.

Yoshikawa **[1986]** suggests several different indices to measure dynamic manipulability based on his previously defined dynamic manipulability ellipsoid. Specifically, "the minimum radius of the dynamic manipulability ellipsoid" is used and evaluated on several simple manipulators. The dynamic manipulability ellipsoid is then applied to arm design in the "specification of the maximum actuator torques." The author concludes that the most useful measure is one that gives the "upper bound of the magnitude of the acceleration with which the end effector can be moved in all directions."

Maciejewski and Klein **[1989]** describe a computationally efficient singular value decomposition (SVD) algorithm for the Jacobian that can be used to optimize manipulability measures in real-time. The point is made that the manipulability measure is popular because it is numerically simple to compute, and its zeros coincide with the singularities of the Jacobian which were previously considered too expensive to compute using SVD.

A modification of the dynamic manipulability ellipsoid presented in Yoshikawa's "Dynamic Manipulability of Robot Manipulators" **[Yoshikawa, 85b]** is presented in Chiacchio et al. **[1992]**. The authors conclude that gravitational forces cause a translation in the ellipsoid and not a "compression" of the volume. This translation means that the "directions of the minimum and maximum acceleration vectors are changed." Now, it can be seen that "the manipulator can accelerate more easily downwards than upwards." Therefore, this new ellipsoid accounts "for the effects of gravity along task space directions in a more correct manner." Adding a payload "reduces the size of the ellipsoid and changes the orientation of its axes." "Translation is reduced when a payload is applied."

Yokokohji and Yoshikawa **[1993]** present a guide for the design of master arms. "By extending the concept of dynamic manipulability, a measure of the manipulating ability of master arms is given." It is stated that the "directional property of the manipulability ellipsoid in the workspace is an important factor." A global measure is also needed, and the standard dynamic manipulability measure satisfies neither condition. A second measure "evaluates the similarity of the manipulability ellipsoids when the operator maneuvers the master arm and when she has no payload." It considers the directional property and can be used to analyze the master arm globally. The new dynamic manipulability measure is constructed under the assumption that the operator arm is grasping another arm (a payload). Therefore the two share a common position and orientation vector. The resulting measure is a function of operator dynamics. Maps are used to show regions where manipulability is high and low. These results can also be used to determine from "which direction the teaching operator should grasp the robot arm." Practical results include that the "weight of master arms should be reduced as much as possible" and that the master arm should be large compared to the operator arm to "remove the singular points from the operator workspace." Several master arms were evaluated using the new measure, and the exoskeleton was found to be the best design. The exoskeleton recommended avoids the singular point problem by having "its singular points coincident with those of the operator arm." This work is not applicable to a slave system interacting with its environment.

The logical extension of this work is to consider the master/slave system instead of only the master arm. This is the basis of teleoperability. The concepts of teleoperability, teleoperability ellipse, teleoperability measure, dynamic teleoperability, dynamic teleoperability ellipse, and dynamic teleoperability measure will provide the telerobotics specialist with a tool to evaluate the ability of a teleoperated or telerobotic slave to reproduce the requested positions and orientations of the master. Evaluation may include examining the uniformity of the measure over the workspace and comparing the magnitude of the measure in different scenarios.

For teleoperability and dynamic teleoperability, typical issues are the same as for manipulability except that instead of comparing a joint space velocity sphere to an end-effector velocity sphere comparisons are made between an “n-sphere” in master end-effector velocity space and an “m-sphere” in slave end-effector velocity space. That is, one looks at how requested motions at the master end-effector are reproduced at the slave end-effector. The next chapter provides the necessary mathematical background to determine teleoperability and dynamic teleoperability ellipses and measures.

3 Mathematical Background

3.1 Teleoperability

The mathematical development starts with the general concept statement for teleoperability. That is, what is the relationship between master end-effector velocity and slave end-effector velocity? The first step is to consider the basic relationship between the end-effector velocity $\mathbf{v}$ (m×1) and the joint velocity $\dot{\mathbf{q}}$ (n×1) for any manipulator. This is expressed by the equation

$$\mathbf{v} = \mathbf{J}(\mathbf{q})\dot{\mathbf{q}} \tag{3.1}$$

where $\mathbf{J}(\mathbf{q})$ is the well-known Jacobian matrix (m×n) described in any basic robotics text. Note that the dependence of $\mathbf{J}$ on the joint angle vector $\mathbf{q}$ will be omitted for notational simplicity for the remainder of this development. The relationship between the joint velocities and the end-effector velocities for both a master (m) and slave (s) manipulator are expressed by

$$\mathbf{v}_m = \mathbf{J}_m \dot{\mathbf{q}}_m \tag{3.2}$$

and

$$\mathbf{v}_s = \mathbf{J}_s \dot{\mathbf{q}}_s . \tag{3.3}$$

In an ideal teleoperated or telerobotic system, the slave motions perfectly follow the master motions; that is, the master and slave joint velocities should be equal for an ideal system. This is expressed by

$$\dot{\mathbf{q}}_m = \dot{\mathbf{q}}_s . \tag{3.4}$$

Note that equation (3.4) implicitly assumes that there are the same number of "free" slave joints (i.e., those that have not been given fixed positions or whose value has not been assigned by some other algorithm) as there are master joints. Dissimilar systems having different numbers of joints in the master and slave will be addressed in the next chapter.

The next step is to solve equation (3.3) for $\dot{\mathbf{q}}_s$ to obtain

$$\dot{\mathbf{q}}_s = \mathbf{J}_s^+ \mathbf{v}_s, \tag{3.5}$$

where $\mathbf{J}_s^+$ is the pseudo-inverse of $\mathbf{J}_s$. Substitute equation (3.5) into equation (3.4) and place the result into equation (3.2) to obtain:

$$\mathbf{v}_m = \mathbf{J}_m \mathbf{J}_s^+ \mathbf{v}_s. \tag{3.6}$$

As stated before, the concept of teleoperability, like manipulability, is to determine the relationship between master end-effector velocity and slave end-effector velocity. Consider the set of master end-effector velocities inside an "n-sphere." Mathematically, this is expressed as:

$$\|\mathbf{v}_m\| \leq 1. \tag{3.7}$$

Since $\mathbf{v}_m$ is a vector,

$$\|\mathbf{v}_m\| = \mathbf{v}_m^T \mathbf{v}_m, \tag{3.8}$$

and therefore

$$\mathbf{v}_m^T \mathbf{v}_m = \mathbf{v}_s^T \left(\mathbf{J}_s^+\right)^T \mathbf{J}_m^T \mathbf{J}_m \mathbf{J}_s^+ \mathbf{v}_s \leq 1. \tag{3.9}$$

If one defines a new Jacobian named the teleoperation Jacobian as

$$\mathbf{J}_{TO} = \mathbf{J}_s \mathbf{J}_m^+, \tag{3.10}$$

then $\|\mathbf{v}_m\| \leq 1$ implies

$$\mathbf{v}_s^T \left(\mathbf{J}_{TO}^{+}\right)^T \mathbf{J}_{TO}^{+} \mathbf{v}_s \leq 1. \tag{3.11}$$

For a vector $\mathbf{r} = (x, y, z)$, $\mathbf{r}^T\mathbf{r} = x^2 + y^2 + z^2 = C$ is a sphere. Therefore, equation (3.11) is the equation of an ellipsoid in the slave manipulator space and represents the mapping of the master end-effector velocity sphere into the slave space. This ellipsoid can be called the teleoperability ellipsoid.

Find the principal axes of the teleoperability ellipsoid through the use of the singular value decomposition (SVD) **[Maciejewski, 89]** of $\mathbf{J}_{TO}$. Let the standard SVD of $\mathbf{J}_{TO}$ be

$$\mathbf{J}_{TO} = \mathbf{U}\Sigma\mathbf{V}^T \tag{3.12}$$

where **U** and **V** are orthogonal, and the non-zero components of Σ are the singular values of $\mathbf{J}_{TO}$. The singular values are defined as the square roots of the nonzero eigenvalues of $\mathbf{J}_{TO}^T\mathbf{J}_{TO}$ and are found in the diagonal entries of

$$\Sigma = \left[\begin{array}{ccccc|c} \sigma_1 & & & & 0 & 0 \\ & \cdot & & & & 0 \\ & & \cdot & & & 0 \\ & & & \cdot & & 0 \\ 0 & & & & \sigma_m & 0 \end{array}\right] \tag{3.13}$$

where $\sigma_1 \geq \sigma_2 \geq \ldots \geq \sigma_m \geq 0$.

If $\mathbf{u}_i$ are the column vectors of **U**, the principal axes of the teleoperability ellipsoid are

$\sigma_1\mathbf{u}_1, \sigma_2\mathbf{u}_2, \ldots, \sigma_m\mathbf{u}_m$.

Similar to the manipulability measure, the volume of the teleoperability ellipsoid can indicate a particular master/slave system or configuration's deviation from ideality. The volume of the teleoperability ellipsoid is proportional to what will be defined as the teleoperability measure (TO_M) where TO_M is given by:

$$TO_M = \sqrt{\det \mathbf{J}_{TO}\mathbf{J}_{TO}^T}\ . \tag{3.14}$$

This measure is equal to the product of the singular values that are the non-zero elements in Σ of the SVD of $\mathbf{J}_{TO} = \mathbf{U}\Sigma\mathbf{V}^T$. In this basic mathematical development, the master and slave were assumed to have equal number of joints; therefore $\mathbf{J}_{TO}$ is square and thus

$$TO_M = \left|\det \mathbf{J}_{TO}\right|. \tag{3.15}$$

Adding robotic capabilities to a teleoperated system impacts teleoperability in two ways. If the telerobot is operated in a purely robotic mode, then teleoperability reduces to manipulability. The master is simply not used. If the telerobotic capabilities are manifested in the form of constraints (e.g., constrained motion along a path, workspace shaping, obstacle avoidance) then teleoperability could be impacted. One could envision scenarios where the slave is constrained and the operator continues to move the master. This would impact teleoperability and could affect performance especially if the master is moved far from alignment with the slave. The next section introduces the theory of dynamic teleoperability.

3.2 Dynamic Teleoperability

Kinematics is concerned with the motion of material bodies while dynamics is concerned with the motion of material bodies under the influence of their surroundings **[Craig, 89]**. Teleoperability only considered the kinematics and not the dynamics of the manipulators. This section introduces the concepts of dynamic teleoperability and the associated dynamic teleoperability measure. Dynamic teleoperability, as its name suggests, does consider the dynamics of the body.

Assume that the manipulator dynamics **[Sciavicco, 00]** of the master are given by

$$\mathbf{M}_m(\mathbf{q}_m)\ddot{\mathbf{q}}_m + \mathbf{h}_m(\mathbf{q}_m, \dot{\mathbf{q}}_m) + \mathbf{g}_m(\mathbf{q}_m) = \tau_m . \qquad (3.16)$$

Note that gravitational forces are included. Similarly, the slave dynamics are given by

$$\mathbf{M}_s(\mathbf{q}_s)\ddot{\mathbf{q}}_s + \mathbf{h}_s(\mathbf{q}_s, \dot{\mathbf{q}}_s) + \mathbf{g}_s(\mathbf{q}_s) = \tau_s . \qquad (3.17)$$

Modify the dynamic equations using $\tilde{\tau} = \tau - \mathbf{h} - \mathbf{g}$, the joint torque compensated for friction, Coriolis, and gravity, which gives $\ddot{\mathbf{q}} = \mathbf{M}^{-1}\tilde{\tau}$. Now, the relationship between end-effector and joint velocity is given by (3.2) for the master and (3.3) for the slave. Differentiating equations (3.2) and (3.3) with respect to time gives, respectively,

$$\dot{\mathbf{v}}_m = \mathbf{J}_m\ddot{\mathbf{q}}_m + \dot{\mathbf{J}}_m\dot{\mathbf{q}}_m \qquad (3.18)$$

and

$$\dot{\mathbf{v}}_s = \mathbf{J}_s\ddot{\mathbf{q}}_s + \dot{\mathbf{J}}_s\dot{\mathbf{q}}_s . \qquad (3.19)$$

Modify the master and slave acceleration terms to include the virtual acceleration resulting from the nonlinear relationship between the joint and end-effector coordinate systems **[Yoshikawa, 86]**. This gives $\tilde{\mathbf{v}} = \dot{\mathbf{v}} - \dot{\mathbf{J}}\dot{\mathbf{q}}$ so $\tilde{\mathbf{v}} = \mathbf{J}\ddot{\mathbf{q}}$. Therefore,

$$\tilde{\mathbf{v}}_m = \mathbf{J}_m \mathbf{M}_m^{-1} \tilde{\tau}_m \tag{3.20}$$

and

$$\tilde{\mathbf{v}}_s = \mathbf{J}_s \mathbf{M}_s^{-1} \tilde{\tau}_s . \tag{3.21}$$

Now the master and slave Jacobians have been modified by multiplication with the inverse of the appropriate inertia matrix.

Next, compare an "n-sphere" in master end-effector acceleration space to an "m-sphere" in slave end-effector acceleration space. The ideal dynamic relationship between the master and slave is for their forces to be equal. This is expressed by

$$\tilde{\tau}_m = \tilde{\tau}_s . \tag{3.22}$$

Note that equation (3.22) implicitly assumes that there are the same number of "free" slave forces (i.e., those that have not been given fixed positions or whose value has not been assigned by some other algorithm) as there are master forces. Equation (3.22) also assumes that the master and slave are under the same gravitational forces. The next step is to solve equation (3.21) for $\tilde{\tau}_s$ to obtain

$$\tilde{\tau}_s = \mathbf{M}_s \mathbf{J}_s^+ \tilde{\mathbf{v}}_s \tag{3.23}$$

where $\mathbf{J}_s^+$ is the pseudo-inverse of $\mathbf{J}_s$. Substitute equation (3.23) into equation (3.22) and place the result into equation (3.20) to obtain

$$\tilde{\mathbf{v}}_m = \mathbf{J}_m \mathbf{M}_m^{-1} \mathbf{M}_s \mathbf{J}_s^+ \tilde{\mathbf{v}}_s . \tag{3.24}$$

As stated before, the concept of dynamic teleoperability, like manipulability, is to determine the relationship between master end-effector acceleration and slave end-effector acceleration. Consider the set of master end-effector accelerations inside an "n-sphere." Mathematically, this is expressed as:

$$\left\|\tilde{\mathbf{v}}_m\right\| \leq 1. \tag{3.25}$$

Since $\tilde{\mathbf{v}}_m$ is a vector,

$$\left\|\tilde{\mathbf{v}}_m\right\| = \tilde{\mathbf{v}}_m^T \tilde{\mathbf{v}}_m, \tag{3.26}$$

and therefore

$$\tilde{\mathbf{v}}_m^T \tilde{\mathbf{v}}_m = \dot{\mathbf{v}}_s^T (\mathbf{J}_s^+)^T \mathbf{M}_s^T (\mathbf{M}_m^{-1})^T \mathbf{J}_m^T \mathbf{J}_m \mathbf{M}_m^{-1} \mathbf{M}_s \mathbf{J}_s^+ \dot{\mathbf{v}}_s \leq 1. \tag{3.27}$$

If one defines a new Jacobian named the dynamic teleoperation Jacobian as

$$\mathbf{J}_{DTO}^+ = \mathbf{J}_m \mathbf{M}_m^{-1} \mathbf{M}_s \mathbf{J}_s^+, \tag{3.28}$$

then $\left\|\tilde{\mathbf{v}}_m\right\| \leq 1$ implies

$$\tilde{\mathbf{v}}_s^T \left(\mathbf{J}_{DTO}^+\right)^T \mathbf{J}_{DTO}^+ \tilde{\mathbf{v}}_s \leq 1. \tag{3.29}$$

Equation (3.29) is the equation of an ellipsoid in the slave manipulator space and represents the mapping of the master end-effector acceleration sphere into the slave space. This ellipsoid can be called the dynamic teleoperability ellipsoid.

Find the principal axes of the dynamic teleoperability ellipsoid through the use of the singular value decomposition (SVD) **[Maciejewski, 89]** of $\mathbf{J}_{DTO}$. Let the standard SVD of $\mathbf{J}_{DTO}$ be

$$\mathbf{J}_{DTO} = \mathbf{U}\Sigma\mathbf{V}^T \tag{3.30}$$

where $\mathbf{U}$ and $\mathbf{V}$ are orthogonal, and the non-zero components of Σ are the singular values of $\mathbf{J}_{DTO}$. The singular values are defined as the square roots of the nonzero eigenvalues of $\mathbf{J}_{DTO}^T\mathbf{J}_{DTO}$ and are the diagonal entrees in

$$\Sigma = \left[\begin{array}{ccccc|c} \sigma_1 & & & & 0 & 0 \\ & \cdot & & & & 0 \\ & & \cdot & & & 0 \\ & & & \cdot & & 0 \\ 0 & & & & \sigma_m & 0 \end{array}\right] \tag{3.31}$$

where $\sigma_1 \geq \sigma_2 \geq \ldots \geq \sigma_m \geq 0$.

If $\mathbf{u}_i$ are the column vectors of $\mathbf{U}$, the principal axes of the dynamic teleoperability ellipsoid are $\sigma_1\mathbf{u}_1, \sigma_2\mathbf{u}_2, \ldots, \sigma_m\mathbf{u}_m$.

Similar to the manipulability measure, the volume of the dynamic teleoperability ellipsoid can indicate a particular master/slave system or configuration's deviation from ideality. The volume of the dynamic teleoperability ellipsoid is proportional to what will be defined as the dynamic teleoperability measure (DTO_M) where DTO_M is given by

$$DTO_M = \sqrt{\det \mathbf{J}_{DTO}\mathbf{J}_{DTO}^T}\,. \tag{3.32}$$

This measure is equal to the product of the singular values that are the non-zero elements in Σ of the SVD of $\mathbf{J}_{DTO} = \mathbf{U}\Sigma\mathbf{V}^T$. In this basic mathematical development, the master and slave were assumed to have equal number of joints; therefore $\mathbf{J}_{DTO}$ is square and thus

$$DTO_M = \left|\det \mathbf{J}_{DTO}\right|. \tag{3.33}$$

The dynamic teleoperability properties can be used for the design of high-bandwidth dexterous teleoperated and telerobotic systems. They could be used to indicate how well a particular master/slave design could reproduce operator motions. They could also be used to impedance match master and slave manipulators for improved performance. The next chapter discusses teleoperability and dynamic teleoperability theory in the context of several common master/slave systems and configurations.

4 Teleoperability and Dynamic Teleoperability for Master/Slave Systems

In this section, the teleoperability and dynamic teleoperability ellipses and measures are examined for various master/slave configurations and operational strategies. Central to this discussion are the common practices of indexing and scaling. Indexing is the intentional misalignment of the master and slave manipulators to enhance operator comfort and task performance. An example would be when an operator is required to work on a task that is mounted to the ceiling of a remote location. She might desire to keep the master manipulator in the horizontal plane to avoid fatigue. In this case, the slave base would be "indexed" $\pi/2$ radians. Indexing might also occur when the operator must avoid joint limits or workspace singularities inherent in the master. Scaling is the introduction of a multiplication factor in the relationship between the master and slave commands or parameters. Scaling can be done either by mechanical design or by algorithms.

4.1 Similar Master/Slave: Scaling--None, Indexing--None

Consider a similar teleoperator system with an unscaled master and slave that are not indexed with respect to each other. The master and slave manipulators will have the same kinematics. Therefore, they have the same Jacobians (i.e., $\mathbf{J}_m = \mathbf{J}_s = \mathbf{J} \in mxn$). Since both the master and the slave have the same Jacobian,

$$\mathbf{J}_{TO} = \mathbf{J}_s \mathbf{J}_m^+ = \mathbf{J}\mathbf{J}^+ \tag{4.1}$$

where $\mathbf{J}_{TO} \in mxm$.

Use the singular-value decomposition (SVD) where $\mathbf{U} \in mxm$, $\Sigma \in mxn$, and $\mathbf{V} \in nxn$, and say

$$\mathbf{J} = \mathbf{U}\Sigma\mathbf{V}^T . \tag{4.2}$$

Therefore,

$$\mathbf{J}\mathbf{J}^+ = \mathbf{U}\Sigma\mathbf{V}^T\mathbf{V}\Sigma^+\mathbf{U}^T . \tag{4.3}$$

Since $\mathbf{V}$ is orthogonal and n x n,

$$\mathbf{V}^T\mathbf{V} = \mathbf{I}^n . \tag{4.4}$$

From the definition of the SVD,

$$\Sigma = \left[\begin{array}{ccc|c} \sigma_1 & & 0 & 0 \\ & \cdot & & 0 \\ & & \cdot & 0 \\ & & \cdot & 0 \\ 0 & & \sigma_m & 0 \end{array}\right] \tag{4.5}$$

where $\sigma_i = \sqrt{\lambda_i}$ where the λ_i are the eigenvalues of $\mathbf{J}^T\mathbf{J}$. So

$$\Sigma^+ = \begin{bmatrix} \sigma_1^{-1} & & & & 0 \\ & \cdot & & & \\ & & \cdot & & \\ & & & \cdot & \\ 0 & & & \cdot & \sigma_m^{-1} \\ - & - & - & - & - \\ & & 0 & & \end{bmatrix} . \tag{4.6}$$

Thus,

$$\Sigma\Sigma^+ = \mathbf{I}^m . \tag{4.7}$$

Therefore,

$$\mathbf{J}\mathbf{J}^+ = \mathbf{I} . \tag{4.8}$$

Since the teleoperator Jacobian, $\mathbf{J}_{TO}$, is the identity matrix (m x m), the teleoperability ellipse from $\|\mathbf{v}_m\| \le 1$ where $\mathbf{v} \in mx1$ implies:

$$\mathbf{v}_s^T \left(\mathbf{J}_{TO}^+\right)^T \mathbf{J}_{TO}^+ \mathbf{v}_s = \mathbf{v}_s^T \mathbf{v}_s = \|\mathbf{v}_s\| \le 1. \tag{4.9}$$

The similar master and slave manipulators will have the same inertia matrices in addition to the same Jacobian. Inertia matrices, $\mathbf{M} \in nxn$ are symmetric by definition. Therefore,

$$\mathbf{J}_{DTO}^+ = \mathbf{J}_m \mathbf{M}_m^{-1} \mathbf{M}_s \mathbf{J}_s^+ = \mathbf{J}\mathbf{M}^{-1}\mathbf{M}\mathbf{J}^+. \tag{4.10}$$

Since for a symmetric matrix A, $\mathbf{A}^{-1}\mathbf{A} = \mathbf{I}$, $\mathbf{J}_{DTO}^+ \in mxm$ reduces to

$$\mathbf{J}_{DTO}^+ = \mathbf{J}\mathbf{J}^+ = \mathbf{I} \tag{4.11}$$

following the argument used previously.

Therefore, $\|\tilde{\mathbf{v}}_m\| \le 1$ where $\tilde{\mathbf{v}} \in mx1$ implies

$$\tilde{\mathbf{v}}_s^T \left(\mathbf{J}_{DTO}^+\right)^T \mathbf{J}_{DTO}^+ \tilde{\mathbf{v}}_s = \tilde{\mathbf{v}}_s^T \tilde{\mathbf{v}}_s \le 1. \tag{4.12}$$

Equation (4.9) states that an "n-sphere" in master end-effector velocity space maps to an "n-sphere" in slave end-effector velocity space. Equation (4.12) states that an "n-sphere" in master end-effector acceleration space maps to an "n-sphere" in slave end-effector acceleration space. This is what one would expect for an ideal, similar teleoperated manipulator system. The teleoperability and dynamic teleoperability measures expressed by equations (3.14) and (3.32) are uniformly equal to 1 throughout the entire workspace of the manipulator system. Because the teleoperability measure is a maximum whenever the master and slave are perfectly aligned, it could be used in a bilateral controller.

ORNL's M2 manipulator system and the ORNL-designed Advanced Servomanipulator (ASM) are examples of this type of teleoperated system **[Kress, 97]**. They perform according to theory within their respective workspaces. That is, the slave exactly reproduces the motions of the master which is expected for kinematic replica systems.

4.2 Similar Master/Slave: Scaling--None, with Indexing

Indexing implies that one can no longer make any general conclusions about the relationship of the master Jacobian, $\mathbf{J}_m$, to the slave Jacobian, $\mathbf{J}_s$. The master and slave could be in any configuration relative to one another; consequently, the teleoperation Jacobian, $\mathbf{J}_{TO}$, and dynamic teleoperation Jacobian, $\mathbf{J}_{DTO}$, will vary. In fact, the slave might move to configurations where it is singular causing the teleoperability and dynamic teleoperability measures to degrade. This could be a problem, for example, if the slave was fully extended but the master was in a non-singular operating position with the operator trying (unsuccessfully) to command the slave to move outward. With remote viewing, where the operator might have difficulty seeing her position, this problem could be compounded. The teleoperability and dynamic teleoperability ellipsoids and teleoperability and dynamic teleoperability measures could vary significantly. This suggests the need for an "emergency return to reference position switch" on indexable master/slave systems. This feature could automatically align the slave with the master so that the operator could return the system to a usable configuration. This must be implemented with appropriate obstacle avoidance capability in order to avoid damaging the remote task space and/or the slave manipulator when the slave manipulator moves autonomously. ORNL's ASM teleoperated system **[Kress, 97]** has indexing capability and also includes such a switch that automatically realigns the slave with the master.

Indexing certain joints, for example the base joint, will not affect the shape of the teleoperability or dynamic teleoperability ellipsoids or the teleoperability or dynamic teleoperability measures. It simply moves the ellipsoid to another position in the workspace. This is mathematically equivalent to a coordinate transformation. However, it will generally not be obvious whether this is true for any particular joint or set of joints at every index position.

4.3 Similar Master/Slave: Scaling--Slave Scaled Uniformly in Length to Master, Indexing--None

A similar teleoperator system with a slave that is scaled uniformly in all link lengths with respect to the master has the following Jacobians **[Sciavicco, 00]** when all of the manipulator joints are revolute:

$$\mathbf{J}_s = \begin{bmatrix} \beta \mathbf{J}_T \\ \cdots \\ \mathbf{J}_R \end{bmatrix} \text{and } \mathbf{J}_m = \begin{bmatrix} \mathbf{J}_T \\ \cdots \\ \mathbf{J}_R \end{bmatrix}, \tag{4.13}$$

where $\mathbf{J}_T \in 3xn$ is the translational part of $\mathbf{J}_m$ and $\mathbf{J}_R \in 3xn$ is the rotational part of $\mathbf{J}_m$ for m = 6. β is the scale factor between the master and the slave. Only $\mathbf{J}_T$ is scaled because the link lengths are only found in the translational components for revolute joints. For the teleoperability measure

$$TO_M = \sqrt{\det \mathbf{J}_{TO}\mathbf{J}_{TO}^T} \tag{4.14}$$

where

$$\mathbf{J}_{TO}\mathbf{J}_{TO}^T = \mathbf{J}_s\mathbf{J}_m^+\left(\mathbf{J}_m^+\right)^T\mathbf{J}_s^T. \tag{4.15}$$

Equation (4.15) is possible because the dimensions of the above matrices are compatible since the manipulators under consideration are similar and results in $\mathbf{J}_{TO}\mathbf{J}_{TO}^T \in mxm$. If dissimilar manipulators were considered, a matrix would be needed to mathematically map between the slave and master.

Since for a matrix $\mathbf{A}$

$$\left(\mathbf{A}^+\right)^T = \left(\mathbf{A}^T\right)^+, \tag{4.16}$$

$$\mathbf{J}_{TO}\mathbf{J}_{TO}^T = \mathbf{J}_s\mathbf{J}_m^+\left(\mathbf{J}_m^T\right)^+\mathbf{J}_s^T. \tag{4.17}$$

Therefore,

$$\mathbf{J}_{TO}\mathbf{J}_{TO}^T = \begin{bmatrix} \beta\mathbf{J}_T \\ \cdots\cdot \\ \mathbf{J}_R \end{bmatrix} \begin{bmatrix} \mathbf{J}_T \\ \cdots\cdot \\ \mathbf{J}_R \end{bmatrix}^+ \left[\mathbf{J}_T^T \;\vdots\; \mathbf{J}_R^T\right]^+ \begin{bmatrix} \beta\mathbf{J}_T \\ \cdots \\ \mathbf{J}_R \end{bmatrix}^T. \tag{4.18}$$

For matrices $\mathbf{A}$ and $\mathbf{B}$,

$$\mathbf{A}^+\mathbf{B}^+ = \left(\mathbf{B}\mathbf{A}\right)^+. \tag{4.19}$$

Therefore,

$$\mathbf{J}_{TO}\mathbf{J}_{TO}^{T} = \begin{bmatrix} \beta\mathbf{J}_{T} \\ \cdots\cdot \\ \mathbf{J}_{R} \end{bmatrix} \left\{ \begin{bmatrix} \mathbf{J}_{T}^{T} & \vdots & \mathbf{J}_{R}^{T} \end{bmatrix} \begin{bmatrix} \mathbf{J}_{T} \\ \cdots \\ \mathbf{J}_{R} \end{bmatrix} \right\}^{+} \begin{bmatrix} \beta\mathbf{J}_{T} \\ \cdots \\ \mathbf{J}_{R} \end{bmatrix}^{T} . \qquad (4.20)$$

Let

$$\mathbf{C} = \left\{ \begin{bmatrix} \mathbf{J}_{T}^{T} & \vdots & \mathbf{J}_{R}^{T} \end{bmatrix} \begin{bmatrix} \mathbf{J}_{T} \\ \cdots \\ \mathbf{J}_{R} \end{bmatrix} \right\}^{+} \qquad (4.21)$$

where $\mathbf{C} \in nxn$.

Now,

$$\mathbf{J}_{TO}\mathbf{J}_{TO}^{T} = \begin{bmatrix} \beta\mathbf{J}_{T}\mathbf{C} \\ \cdots \\ \mathbf{J}_{R}\mathbf{C} \end{bmatrix}^{mxn} \begin{bmatrix} \beta\mathbf{J}_{T}^{T} & \vdots & \mathbf{J}_{R}^{T} \end{bmatrix}^{nxm} \qquad (4.22)$$

or

$$\mathbf{J}_{TO}\mathbf{J}_{TO}^{T} = \begin{bmatrix} \beta^{2}\left(\mathbf{J}_{T}\mathbf{C}\mathbf{J}_{T}^{T}\right) & \vdots & \beta\left(\mathbf{J}_{T}\mathbf{C}\mathbf{J}_{R}^{T}\right) \\ \cdots & \vdots & \cdots \\ \beta\left(\mathbf{J}_{R}\mathbf{C}\mathbf{J}_{T}^{T}\right) & \vdots & \left(\mathbf{J}_{R}\mathbf{C}\mathbf{J}_{R}^{T}\right) \end{bmatrix} \qquad (4.23)$$

where

$$TO_{M} = \sqrt{\det \mathbf{J}_{TO}\mathbf{J}_{TO}^{T}} . \qquad (4.24)$$

This result can be found from an extension of the standard matrix property for a nxn matrix **A** multiplied by a scalar α

$$\det(\alpha\mathbf{A}) = \alpha^{n} \det \mathbf{A} . \qquad (4.25)$$

Extending this property to the present case gives

$$\det\left(\left(\mathbf{J}_{TO}\mathbf{J}_{TO}^{T}\right)_{scaled}\right) = \beta^{2N} \det\left(\mathbf{J}_{TO}\mathbf{J}_{TO}^{T}\right)_{unscaled} \qquad (4.26)$$

where N is the rank of the translation component, $\mathbf{J}_T$,of the slave .

Since section 4.1 gives

$$\det\left(\mathbf{J}_{TO}\mathbf{J}_{TO}^T\right)_{unscaled} = 1, \qquad (4.27)$$

$$\det\left(\left(\mathbf{J}_{TO}\mathbf{J}_{TO}^T\right)_{scaled}\right) = \beta^{2N}. \qquad (4.28)$$

Therefore the teleoperability measure is

$$TO_m = \sqrt{\det\left(\left(\mathbf{J}_{TO}\mathbf{J}_{TO}^T\right)_{scaled}\right)} = \sqrt{\beta^{2N}} = \beta^N. \qquad (4.29)$$

The measure would have an inverse result if the master were scaled instead of the slave.

The basis for N factoring into this result can be seen when the development is split into the translational and rotational parts. For the translational part, (subscript T denotes just the translational portions of **J** and **v**):

$$\mathbf{J}_{TO_T} = \beta\mathbf{J}_{s_T}\mathbf{J}_{m_T}^+ = \beta\mathbf{J}_T\mathbf{J}_T^+ \qquad (4.30)$$

where $\mathbf{J}_{TO_T} \in 3x3$ and $\mathbf{J}_T \in 3xn$.

Scaling of prismatic joints affects neither the rotational nor the translational portion of the Jacobian **[Sciavicco,00]**. Following the same mathematical derivation for prismatic joints as was followed for equations 4.13 through 4.28, the result of equation 4.28 holds if 2N is replaced by 2(N-P) where P is the number of prismatic joints present. For example, if all of the joints were prismatic (i.e., N equaled P), then scaling would have no effect on the Jacobian or the teleoperability measure which agrees with intuition.

The ensuing mathematical development parallels that previously described but now includes the scale factor term. $\left\|\mathbf{v}_{m_T}\right\| \leq 1$ where $\mathbf{v}_T \in 3x1$ implies

$$\beta^2 \mathbf{v}_{s_T}^T \mathbf{v}_{s_T} \leq 1. \tag{4.31}$$

Equation (4.31) states that an "n-sphere" in master end-effector translational velocity space maps to a scaled "n-sphere" in slave end-effector translational velocity space. The teleoperability measure expressed by equations (3.14) and (3.15) is

$$TO_m = \sqrt{\det(\mathbf{J}_{TO_T}\mathbf{J}_{TO_T}^T)} = \sqrt{\det(\beta^2 \mathbf{J}\mathbf{J}^+\mathbf{J}\mathbf{J}^+)}\ . \tag{4.32}$$

Since $\mathbf{J}\mathbf{J}^+ = \mathbf{I}$,

$$TO_m = \sqrt{\det(\beta^2 \mathbf{I})} = \sqrt{\beta^{2n}} \tag{4.33}$$

is uniformly equal to $\sqrt{\beta^{2n}} = \beta^n$ where n is the rank of $\mathbf{J}_{TO_T}$ since $\det(\alpha\mathbf{A}) = \alpha^n \det(\mathbf{A})$ for a matrix $\mathbf{A}$ of rank n. For the rotational part (subscript R denotes just the rotational portions of **J** and **v**) one obtains:

$$\mathbf{J}_{TO_R} = \mathbf{J}_R \mathbf{J}_R^+ \tag{4.34}$$

where $\mathbf{J}_{TO_R} \in 3x3$.

The ensuing mathematical development parallels that of section 3.1. $\left\|\mathbf{v}_{m_R}\right\| \leq 1$ where $\mathbf{v}_R \in 3x1$ implies

$$\mathbf{v}_{s_R}^T \mathbf{v}_{s_R} \leq 1. \tag{4.35}$$

Equation (4.35) states that an "n-sphere" in master end-effector rotational velocity space maps to an unscaled "n-sphere" in slave end-effector rotational velocity space.

This is an interesting conclusion and says that the relationship between slave and master translational velocities is not the same as the relationship between the slave and master rotational velocities. This is what is desired for some tasks but this may not be universally desired. If one wants to preserve the relationship between translational and rotational velocities, then one must introduce a scale factor on the rotational velocities for scaled, replica master/slave teleoperators.

Schilling™ teleoperated manipulators normally come with a scaled miniature replica master manipulator. These arms were used in the dual arm work module and the dual arm work platform design and built at ORNL **[Kress, 97]**. The effect of the scale factor, β, in equation (4.33) has been observed in tasks requiring high precision. When an operator performs precise tasks with a scaled miniature master, she will often experience difficulty having sufficient musculo-skeletal resolution with the teleoperated system. Mathematical scale factors must then be introduced.

Following a similar development, the effect of uniform length scaling on the dynamic teleoperability measure can also be determined for revolute arms. Paralleling the teleoperability development, the slave lengths will be uniformly scaled. The dynamic teleoperability measure consists of the Jacobian and mass matrices for the master and slave. The Jacobians are once again scaled according to (4.23) while the effect of length scaling on the mass matrices is determined to be

$$\mathbf{M}_s = \beta^2 \mathbf{M}_m . \tag{4.36}$$

Following the mathematical development for the teleoperability measure results in

$$\det\left(\left(\mathbf{J}_{DTO}\mathbf{J}_{DTO}^T\right)_{scaled}\right) = \frac{1}{\beta^2}\det\left(\mathbf{J}_{DTO}\mathbf{J}_{DTO}^T\right)_{unscaled} . \tag{4.37}$$

As was done for the teleoperability measure, the dynamic teleoperability measure can then be found from

$$\det(\alpha\mathbf{A}) = \alpha^n \det\mathbf{A} \tag{4.38}$$

for a nxn **A**.

$$DTO_m = \sqrt{\det\left(\left(\mathbf{J}_{DTO}\mathbf{J}_{DTO}^T\right)_{scaled}\right)} = \sqrt{\frac{1}{\beta^{2m}}} = \frac{1}{\beta^m} \tag{4.39}$$

for a mxm $\left(\mathbf{J}_{DTO}\mathbf{J}_{DTO}^T\right)_{unscaled}$. The number of velocity components in the operational space under consideration is m. For example, a 3 DOF planar arm would have m equal to 3 because of x and y translational velocities and the rotational velocity.

4.4 Similar Master/Slave: Scaling--Slave Scaled Non-Uniformly in Length to Master, Indexing--None

Non-uniformly scaling the slave manipulator (e.g., having one link of the slave have a length half that of the corresponding link on the master manipulator with all other links the same length as their respective master links) represents the same problem as indexing.

General conclusions cannot be made about the teleoperability and dynamic teleoperability ellipses and measures.

4.5 Similar Master/Slave: Scaling--Slave Scaled Uniformly in Mass to Master, Indexing--None

The teleoperability measure is not dependent on the mass of the links. Therefore, it is unaffected by mass scaling. The dynamic teleoperability measure, however, is dependent on the mass of the manipulator links. The dynamic teleoperability measure was defined in (3.32). Therefore, with mass scaling

$$\mathbf{J}_s = \mathbf{J}_m . \tag{4.40}$$

For all manipulators, the mass matrix is determined from **[Sciavicco, 00]** by

$$\mathbf{B}(\mathbf{q}) = \sum_{i=1}^{n} m_{l_i} \mathbf{J}_T^{(l_i)T} \mathbf{J}_T^{(l_i)} \tag{4.41}$$

when the masses or the rotors of the joint motors, the moments of inertia with respect to the axes of the rotors, and the moments of inertia relative to the centers of mass of the links are neglected. In (4.41), m_{l_i} are the masses of the links. Therefore if every mass is scaled by γ, the scaled mass matrix is

$$\mathbf{B}_{scaled}(\mathbf{q}) = \sum_{i=1}^{n} \gamma m_{l_i} \mathbf{J}_T^{(l_i)T} \mathbf{J}_T^{(l_i)} . \tag{4.42}$$

Therefore,

$$\mathbf{B}_{scaled}(\mathbf{q}) = \gamma \mathbf{B}_{unscaled}(\mathbf{q}) \tag{4.43}$$

or

$$\mathbf{M}_s = \gamma \mathbf{M}_m \tag{4.44}$$

gives

$$\det\left(\left(\mathbf{J}_{DTO}\mathbf{J}_{DTO}^T\right)_{scaled}\right) = \frac{1}{\gamma^2}\det\left(\mathbf{J}_{DTO}\mathbf{J}_{DTO}^T\right)_{unscaled}. \tag{4.45}$$

As when the lengths of the slave links were uniformly scaled, the dynamic teleoperability measure can then be found from (4.38)

$$DTO_m = \sqrt{\det\left(\left(\mathbf{J}_{DTO}\mathbf{J}_{DTO}^T\right)_{scaled}\right)} = \sqrt{\frac{1}{\gamma^{2m}}} = \frac{1}{\gamma^m} \tag{4.46}$$

for a mxm $\left(\mathbf{J}_{DTO}\mathbf{J}_{DTO}^T\right)_{unscaled}$.

4.6 Similar Master/Slave: Scaling--Slave Scaled Non-Uniformly in Mass to Master, Indexing--None

Non-uniformly mass scaling the slave manipulator (e.g., having one link of the slave have a mass half that of the corresponding link on the master manipulator with all other links the same mass as their respective master links) represents the same problem as indexing and length scaling. One cannot make general conclusions about the teleoperability and dynamic teleoperability Jacobians and the teleoperability and dynamic teleoperability ellipses and measures.

4.7 Velocity Scaling or Workspace Mapping between Similar Master and Slave

Scaling the master velocities in an algorithm rather than mechanically could adversely affect the teleoperability and dynamic teleoperability as it did with indexing. This results from the slave and master eventually losing track of one another as time progresses. Workspace mapping could also adversely affect teleoperability and dynamic teleoperability in a similar way. The slave could be constrained while the operator continues to command the master to move. This would impact teleoperability and dynamic teleoperability and could affect the teleoperability and dynamic teleoperability measures, especially if the master is moved far from alignment with the slave.

4.8 Force Reflection

In force reflection theory,

$$\tilde{\tau}_m = \delta \tilde{\tau}_s \tag{4.47}$$

where δ is the force reflection ratio. Force reflection will only affect the dynamic teleoperability measure where the dynamics are a factor. Therefore,

$$DTO_m = \sqrt{\det\left(\left(\delta^2 \mathbf{J}_{DTO}\mathbf{J}_{DTO}^T\right)_{unscaled}\right)} = \sqrt{\delta^{2m}} = \delta^m \tag{4.48}$$

for a mxm $\left(\mathbf{J}_{DTO}\mathbf{J}_{DTO}^T\right)_{unscaled}$. This result indicates that it would be difficult to draw conclusions about different systems or operational modes by only comparing numerical values of the dynamic teleoperability measure since so many factors can alter the measure. Instead, the variation of the measure across a workspace or along a path would provide a more realistic representation of dynamic teleoperability. An application of this concept will be presented in chapter 7.

4.9 Dissimilar Master/Slave and Cartesian-Based Controllers

Dissimilar teleoperated systems might have dissimilar lengths or dissimilar numbers of joints. For dissimilar master and slave teleoperators, the master Jacobian, $\mathbf{J}_m$, and the slave Jacobian, $\mathbf{J}_s$, must be modified to include the controller kinematics that resolve the differences between the kinematic configurations. This implies that the teleoperability and dynamic teleoperability ellipsoids and measures should include the mathematical mapping between master and slave joint spaces. This suggests that optimizing the teleoperability and dynamic teleoperability measures might be one method to develop an alternative controller for dissimilar teleoperator systems. For example, a control scheme could be created that maximizes the uniformity of the teleoperability or dynamic teleoperability measure in a given region.

Dissimilar teleoperator systems often use Cartesian-based controllers. If one considers an ideal teleoperated system with an ideal controller, then Cartesian controllers that pass direct velocity commands from the master to the slave are a trivial case to consider from a teleoperability viewpoint. An "n-sphere" in master end-effector velocity space maps to an "n-sphere" in slave end-effector velocity space. This, however, is predicated on the assumption that an ideal controller exists for the slave that perfectly produces the requested velocity or acceleration commands. Real systems are not ideal, and both the manipulators and controllers have dynamic responses. Including manipulator dynamics in the teleoperability analysis has already been discussed in the dynamic teleoperability presentation. Controller kinematics and dynamics can be included in the teleoperability analysis as well. This would be necessary for an analysis of a Cartesian-based controller.

One problem observed in the operation of teleoperators that rely on Cartesian-based control schemes is that correspondence is not always maintained between the master and the slave. Even if the master Cartesian commands are executed properly by the slave, the slave motion required to achieve the Cartesian commands may not be what was desired or intended, especially for highly dissimilar systems. Approach directions and arm orientation often change in undesirable ways. These changes would be reflected in a variation in the teleoperability or dynamic teleoperability measure for these conditions.

4.10 Velocity (or Joystick-Type) Controllers

Velocity based controllers such as joysticks that are programmed to send Cartesian velocity commands will appear similar to Cartesian-based controllers from a teleoperability viewpoint. However, when dynamic teleoperability is considered, joystick-type controllers are much different. Velocity based controllers that are programmed to send joint velocity commands will have problems like those of a master/slave system with indexing from a teleoperability viewpoint. The slave will be able to be driven into singularities and the operator might not necessarily be aware of the potential problem. This is generally acceptable for large, slow-moving systems because the operator has ample time to respond to problem configurations.

4.11 Position-Force Controllers

Position-force controlled teleoperator systems such as those pioneered by Carl Flateau **[Flateau, 65]** would also benefit from a teleoperability-like analysis. When the feedback loop from the slave to the master is analyzed, the relationship between torque and force given by

$$\tau = \mathbf{J}^T \mathbf{f} \tag{4.49}$$

where $\tau \in nx1$ is the joint torque and $\mathbf{f} \in mx1$ is the end-effector force will be included in the teleoperability analysis along with the kinematic and controller relationships. Experience with position-force teleoperated systems **[Jansen, 96]** has shown that, similar to scaled master manipulators, force transducers in the control loop can introduce problems because of signal resolution and noise. A smoothing control signal derived from a kinematic based measure such as the teleoperability measure or one based on dynamic properties but not relying on the force transducer signals might help to reduce the effects of noise or load disturbances.

4.12 Mapping Master to Slave

In the case of a redundant master/slave system or when a system has coupled motors, a mapping will exist between the master and slave that is given by

$$\mathbf{A}\mathbf{q}_m = \mathbf{q}_s . \tag{4.50}$$

$\mathbf{A}$ is a linear representation of the mapping from the master to the slave. This relationship gives

$$\dot{\mathbf{q}}_m = \mathbf{A}^+\dot{\mathbf{q}}_s . \tag{4.51}$$

Thus $\mathbf{v}_m = \mathbf{J}_m\dot{\mathbf{q}}_m$ becomes

$$\mathbf{v}_m = \mathbf{J}_m\mathbf{A}^+\mathbf{J}_s^+\mathbf{v}_s . \tag{4.52}$$

From the formation of the teleoperability ellipsoid (3.9), a new teleoperability measure can be defined as

$$\mathbf{J}_{TO_{mapping}} = \mathbf{J}_s\mathbf{A}\mathbf{J}_m^+ . \tag{4.53}$$

The modified teleoperability measure can then be found from

$$TO_{m_{mapping}} = \sqrt{\det J_{TO_{mapping}} J_{TO_{mapping}}^T} . \tag{4.54}$$

5 Teleoperability and Dynamic Teleoperability Simulations

In this chapter, teleoperability and dynamic teleoperability results are presented for simple 2 and 3 DOF systems. These systems are used for simulation purposes only since a realistic teleoperated system would have at least 5 to 6-DOF per manipulator arm or master controller. Presented results include the effect of indexing, length scaling, and mass scaling. The teleoperated systems were simulated in Matlab™. The theoretical developments of chapters 3 and 4 have been verified numerically using these simulations.

5.1 Teleoperability Simulations

This section presents teleoperability results for a three-degree-of-freedom planar master/slave teleoperated system with indexing and length scaling. Mass scaling does not affect the teleoperability measure since the dynamics of the system are not considered. The system is shown in Figure 5.1. The demonstrative teleoperated system is capable of producing an arbitrary position and orientation within the planar area of its reachable space.

The Jacobians of the master and slave are needed for the calculation of the teleoperability measure. The Jacobian matrix **[Yoshikawa, 90]** for the 3-DOF planar manipulator is

$$\mathbf{J} = \begin{bmatrix} -(l_1 S_1 + l_2 S_{12} + l_3 S_{123}) & -(l_2 S_{12} + l_3 S_{123}) & -l_3 S_{123} \\ l_1 C_1 + l_2 C_{12} + l_3 C_{123} & l_2 C_{12} + l_3 C_{123} & l_3 C_{123} \\ 1 & 1 & 1 \end{bmatrix}. \qquad (5.1)$$

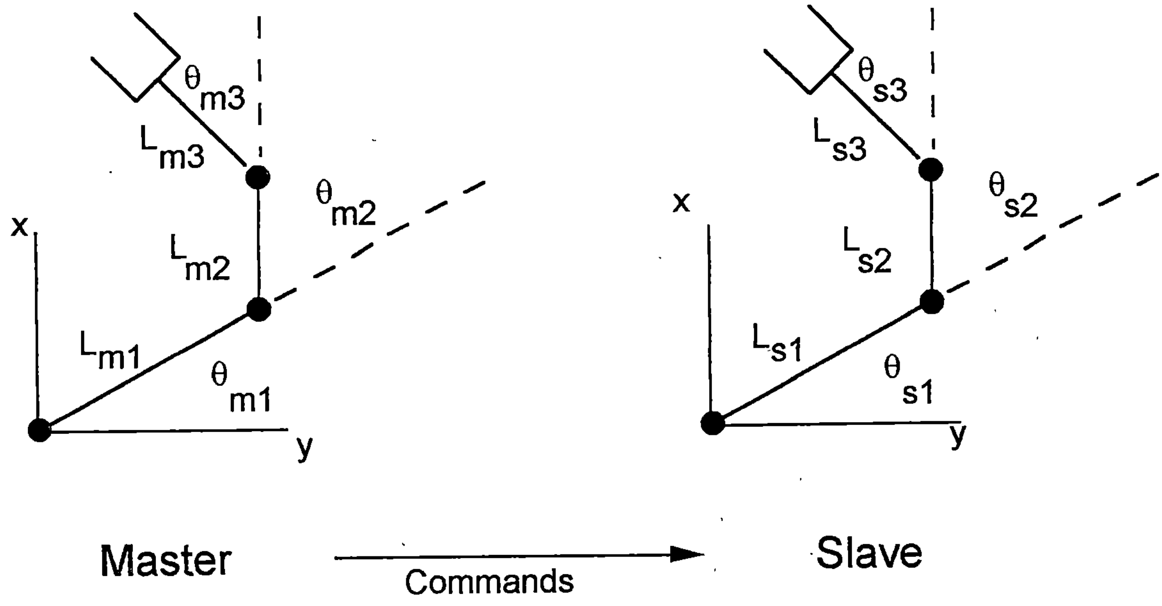

Figure 5.1: 3-DOF, planar teleoperated system.

In equation (5.1), S_i is the sine of joint angle i, C_i is the cosine of joint angle i, and a term such as S_{ij} is the sine of the sum of joint angles i and j. The length of the i^{th} link is l_i.

Calculation of the Jacobian requires knowledge of the joint angles. Given a desired position and orientation in the (x,y) plane defined by (x,y, ϕ), the joint angles of the 3-DOF planar manipulator can be found using the inverse kinematic solution **[Craig, 89]**.

1) Calculate θ_2 between 0 and π from its cosine, $c_2 = \frac{x^2+y^2-l_1^2-l_2^2}{2l_1l_2}$.

2) Define intermediate variables, β = Atan2(x,y) and

$\cos\psi = \left(x^2+y^2+l_1^2-l_2^2\right)/\left(2l_1\sqrt{x^2+y^2}\right)$ for ψ between 0 and π to obtain joint angle 1,

$\theta_1 = \beta \pm \psi$.

3) From $\theta_1+\theta_2+\theta_3=\phi$, calculate joint angle 3.

5.1.1 Indexing

Figure 5.2 illustrates the workspace of the simulation based on the similar, 3-DOF, planar master/slave teleoperated system with indexing but no scaling between the master and slave. The simulated master was moved in the square $0.8 \le x \le 1.2$, $0.8 \le y \le 1.2$ and the simulated slave was commanded to maintain a 0-radians orientation with respect to the x-axis. The teleoperability measure for the system was evaluated for three different operational scenarios.

A) No indexing between the master and slave

B) The slave base indexed $\pi/2$

C) The slave base and slave second joint indexed $\pi/4$

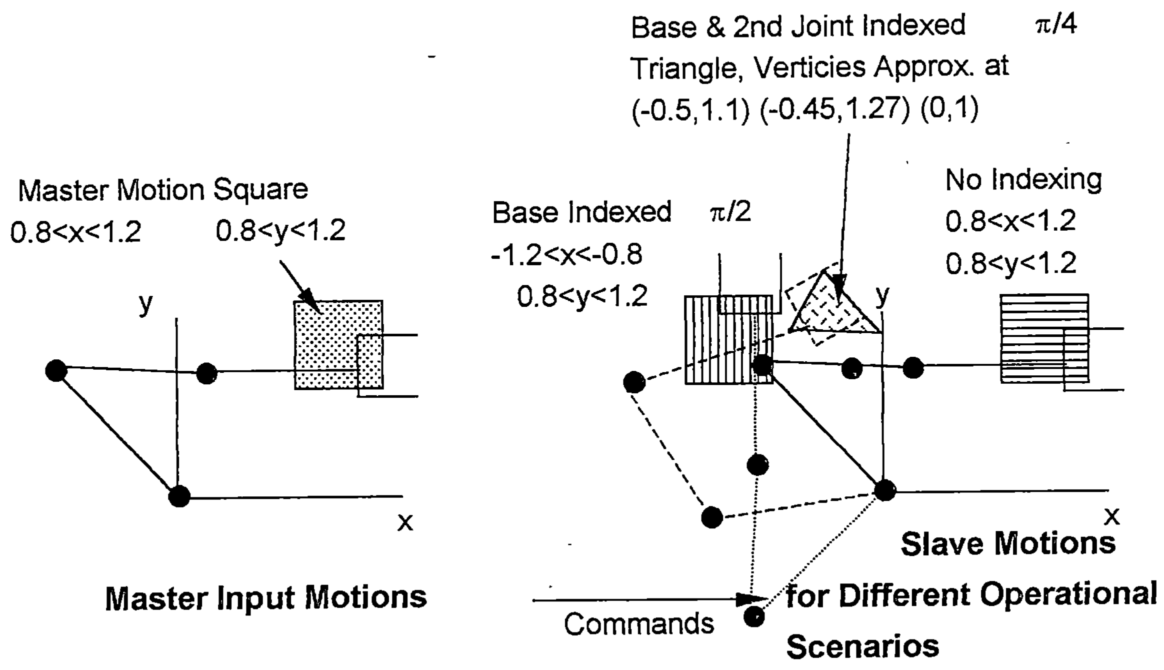

Figure 5.2: Simulated workspace motion for indexing.

In the slave space, the square from $0.8 \le x \le 1.2$, $0.8 \le y \le 1.2$ is associated with the no indexing case, the square from $-1.2 \le x \le -0.8$, $0.8 \le y \le 1.2$ is associated with the base indexed $\pi/2$, and the triangle (approximate shape) is associated with the base and second joint indexed $\pi/4$.

Figure 5.3 is a three-dimensional plot of the simulated motions illustrated in Figure 5.2. The (x,y) plane is the slave task space plane, and the z-axis is the teleoperability measure for each point in the slave task space. All three operational scenarios are shown.

First, consider the slave task space square associated with the no indexing case. The teleoperability theory asserts that the teleoperability measure should be 1.0 throughout slave workspace. It is, as is seen by the value of the teleoperability measure in the square at $0.8 \le x \le 1.2$, $0.8 \le y \le 1.2$. The "rotated square," located at $-1.2 \le x \le -0.8$, $0.8 \le y \le 1.2$ is associated with the base indexed $\pi/2$. For this case, teleoperability theory states that the teleoperability measure should be 1.0 throughout slave workspace. As before, the value of the teleoperability measure in this square is uniformly 1.0. Finally, consider the slave task space associated with the base and second joint indexed $\pi/4$. This is the triangle (approximate shape) in Figure 5.2. The teleoperability theory for this operational scenario states that the teleoperability measure can vary unpredictably if the indexed slave approaches a singularity. This is seen to be the case in Figure 5.3 where the teleoperability measure is decreasing towards 0 when the slave is attempting to reach the point (0,1).

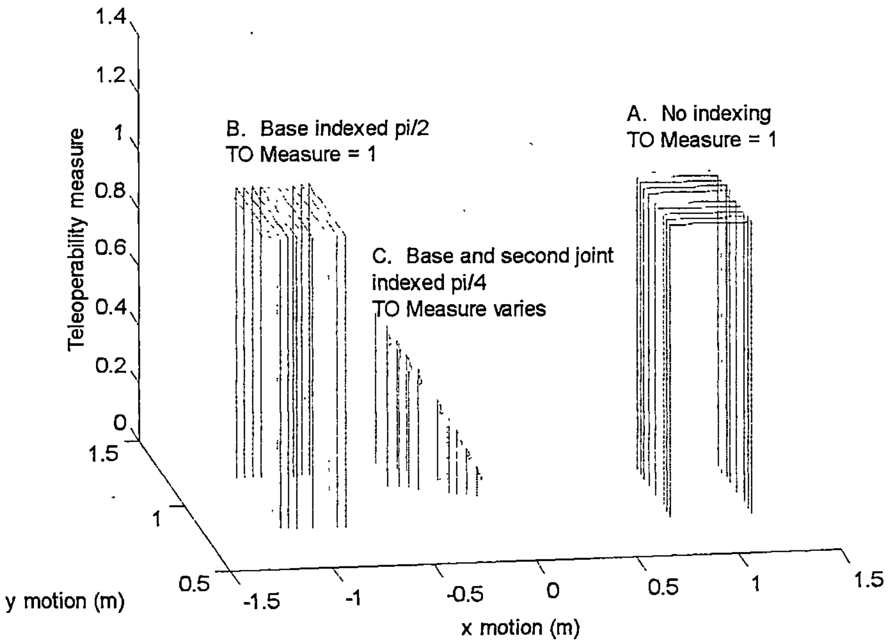

Figure 5.3: Teleoperability measure in the slave task space from indexing the slave. The vertical lines are for placement only and do not show the measure going to zero at the edges of the workspaces.

5.1.2 Length Scaling

The teleoperability measure for the system was evaluated for three different length scaling scenarios.

A) No length scaling between the master and slave (scaling factor $\beta = 1$)

B) The slave lengths scaled to twice the master lengths (scaling factor $\beta = 2$)

C) The slave lengths scaled to 1/3 the master lengths (scaling factor $\beta = 1/3$)

Figure 5.4 is a three-dimensional plot of these scenarios. The (x,y) plane is the slave task space plane, and the z-axis is the teleoperability measure for each point in the slave task space.

First, consider the slave task space square associated with the no scaling case. The teleoperability theory asserts that the teleoperability measure should be 1.0 throughout slave workspace. It is, as shown by case A in Figure 5.4. Since no indexing occurred, the slave workspace is the same as the master workspace of $0.8 \le x \le 1.2$, $0.8 \le y \le 1.2$ for all three scenarios. As predicted by the teleoperability theory, when the slave lengths are scaled by a factor β, the teleoperability measure will be β^N where N is the rank of the translational component of the Jacobian as described in section 4.3. For the 3-DOF planar manipulator, the rank of the translational component is 2, and the measure agrees and is calculated to be β^2 as shown in cases A, B, and C.

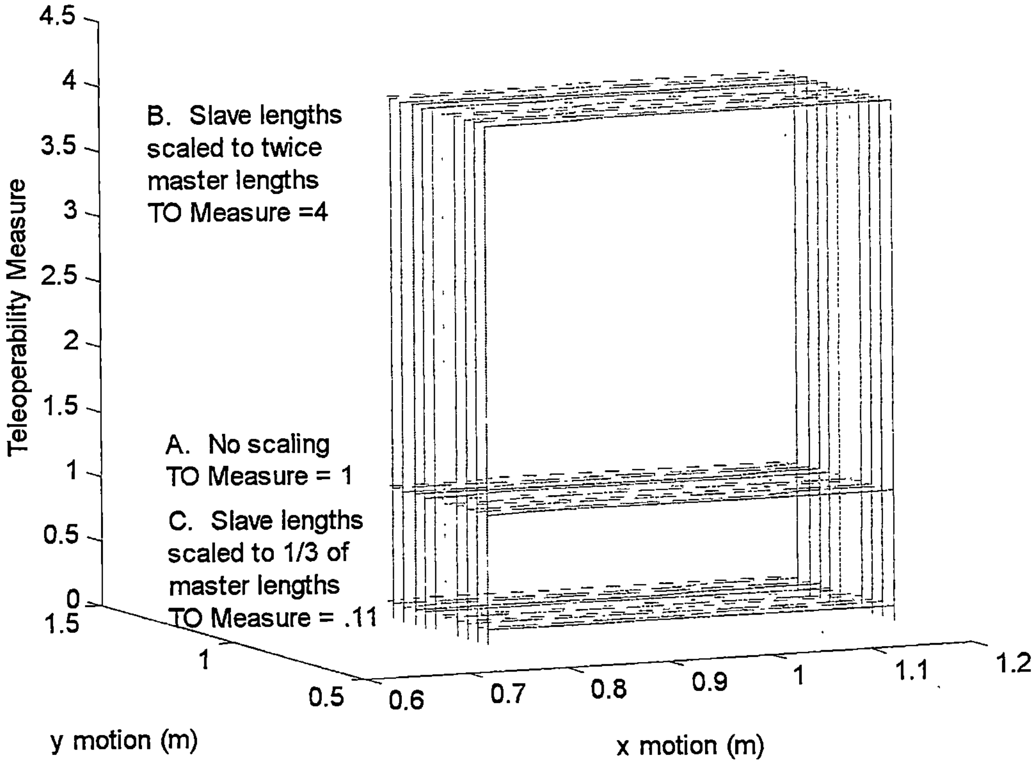

Figure 5.4: Teleoperability measure in the slave task space from length scaling the slave. The vertical lines are for placement only and do not show the measure going to zero at the edges of the workspaces.

5.2 Dynamic Teleoperability Simulations

This section presents dynamic teleoperability results for a 2-DOF planar master/slave teleoperated system that includes indexing, length scaling, and mass scaling. The system is shown in Figure 5.5. The Jacobians and inertia matrices of the master and slave are needed for the calculation of the dynamic teleoperability measure. The Jacobian matrix for the 2-DOF planar arm is

$$\mathbf{J} = \begin{bmatrix} -(l_1 S_1 + l_2 S_{12}) & -l_2 S_{12} \\ l_1 C_1 + l_2 C_{12} & l_2 C_{12} \end{bmatrix}. \qquad (5.2)$$

In equation (5.2), S_i is the sine of joint angle i, C_i is the cosine of joint angle i, and a term such as S_{ij} is the sine of the sum of joint angles i and j. The length of the i^{th} link is l_i.

Calculation of the Jacobian requires knowledge of the joint angles. Given a desired position and orientation in the (x,y) plane defined by (x,y, ϕ), the solution for the joint angles of the 2-DOF planar manipulator can be found using the inverse kinematics solution **[Craig, 89]**.

1) Define an intermediate variable $\kappa = \sqrt{\left(x^2+y^2+l_1^2+l_2^2\right)^2 - 2\left(\left(x^2+y^2\right)^2 + l_1^4 + l_2^4\right)}$.

2) Calculate joint angle 1, θ_1, from $\theta_1 = a\tan2(y,x) - a\tan2(\kappa, x^2+y^2+l_1^2-l_2^2)$.

3) Calculate joint angle 2, θ_2, from $\theta_2 = a\tan2(\kappa, x^2+y^2-l_1^2-l_2^2)$.

The inertia matrix for a 2-DOF planar manipulator needed for the dynamic teleoperability measure is

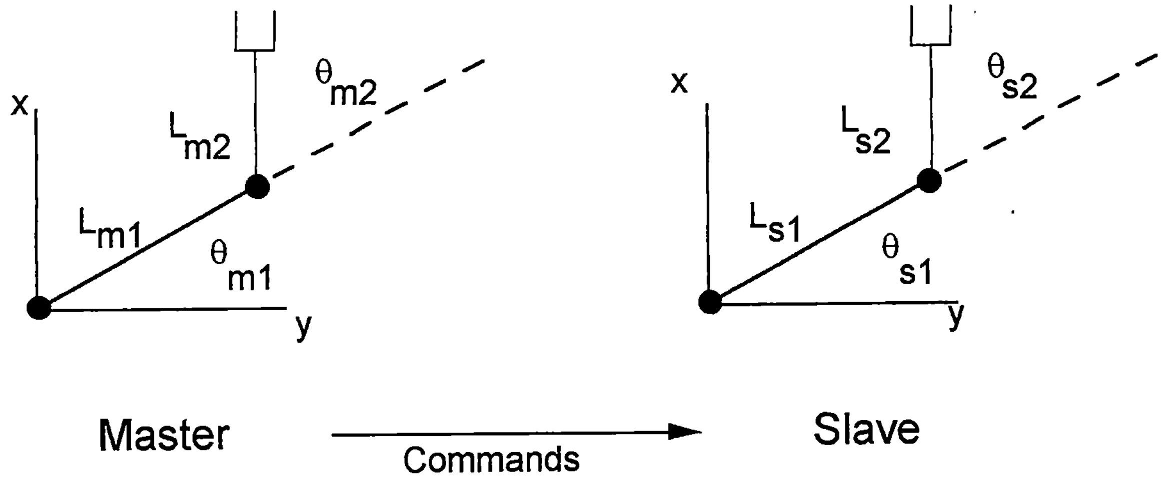

Figure 5.5: 2-DOF, planar teleoperated system.

$$\mathbf{M} = \begin{bmatrix} m_1(l_{c_1}^2 + m_2(l_1^2 + l_{c_2}^2 + 2l_1 l_{c_2} C_2 & m_2(l_{c_2}^2 + l_1 l_{c_2} C_2) \\ m_2(l_{c_2}^2 + l_1 l_{c_2} C_2) & m_2 l_{c_2}^2 \end{bmatrix} \quad (5.3)$$

when the masses of the rotors, the moments of inertia relative to the center of mass of the links, and the moments of inertia with respect to the axes of the slave rotors are neglected.

5.2.1 Indexing

The simulated master was moved in the square $0.8 \leq x \leq 1.2$, $0.8 \leq y \leq 1.2$, and the simulated slave was commanded to maintain a 0-radians orientation with respect to the x-axis. Figure 5.6 illustrates the slave workspace that results from the indexing simulations. In this simulation, there was no scaling between the master and slave. The dynamic teleoperability measure for the system was evaluated for three different operational scenarios.

A) No indexing between the master and slave

B) The slave base indexed $\pi/2$

C) The slave base and slave second joint indexed $\pi/4$

Figure 5.7 is a three-dimensional plot of the simulated motions illustrated in Figure 5.2. The (x,y) plane is the slave task space plane, and the z-axis is the dynamic teleoperability measure for each point in the slave task space. All three operational scenarios are shown.

First, consider the slave task space square associated with the no indexing case. The dynamic teleoperability theory asserts that the dynamic teleoperability measure should be

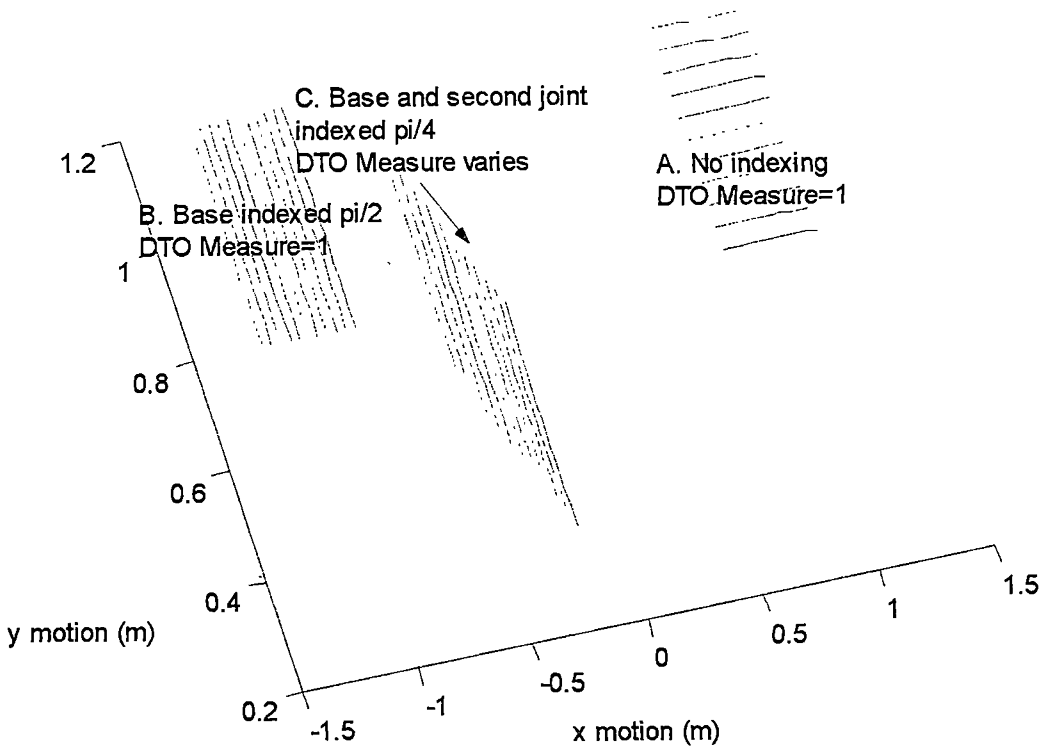

Figure 5.6: Slave workspace from indexing simulation.

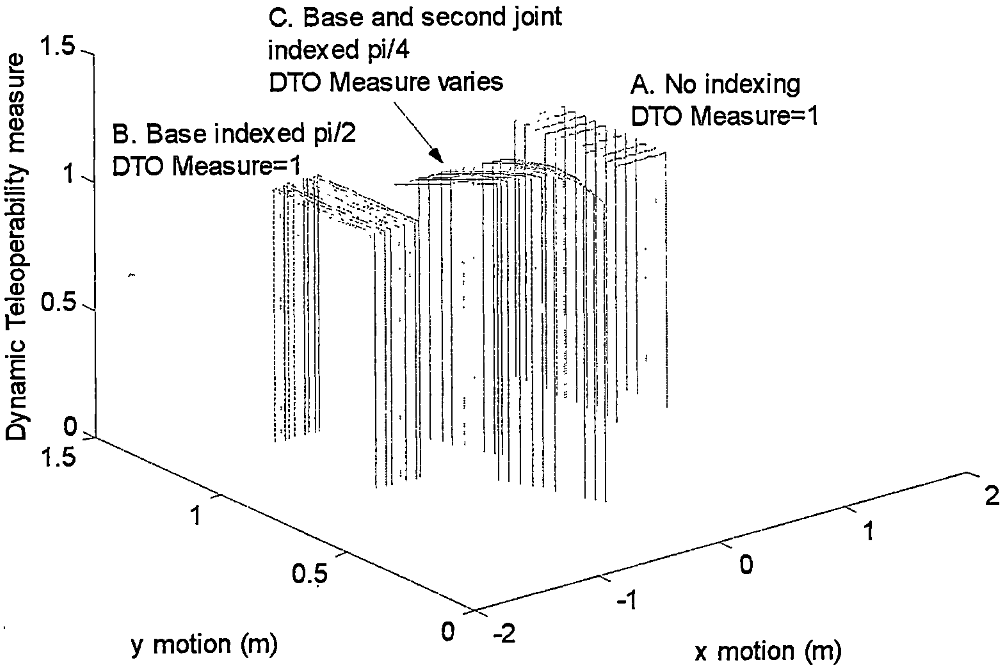

Figure 5.7: Dynamic teleoperability measure in the slave task space from indexing the slave. The vertical lines are for placement only and do not show the measure going to zero at the edges of the workspaces.

1.0 throughout the slave workspace. It is, as is seen by the value of the dynamic teleoperability measure in the square at $0.8 \le x \le 1.2$, $0.8 \le y \le 1.2$.

The "rotated square," located at $-1.2 \le x \le -.8$, $0.8 \le y \le 1.2$ is associated with the base indexed $\pi/2$. For this case, dynamic teleoperability theory states that the dynamic teleoperability measure should be 1.0 throughout the slave workspace. As before, the value of the dynamic teleoperability measure in this square is uniformly 1.0. Finally, consider the slave task space associated with the base and second joint indexed $\pi/4$. This is the parallelogram (approximate shape) in Figure 5.6. The dynamic teleoperability theory for this operational scenario states that the dynamic teleoperability measure can vary. This is seen to be the case in Figure 5.7.

5.2.2 Length Scaling

The dynamic teleoperability measure for the system was evaluated for three different length scaling scenarios.

A) No length scaling between the master and slave (scaling factor $\beta = 1$)

B) The slave lengths scaled to twice the master lengths (scaling factor $\beta = 2$)

C) The slave lengths scaled to 1/3 the master lengths (scaling factor $\beta = 1/3$)

Figure 5.8 is a three-dimensional plot of these scenarios. The (x,y) plane is the slave task space plane, and the z-axis is the dynamic teleoperability measure for each point in the slave task space.

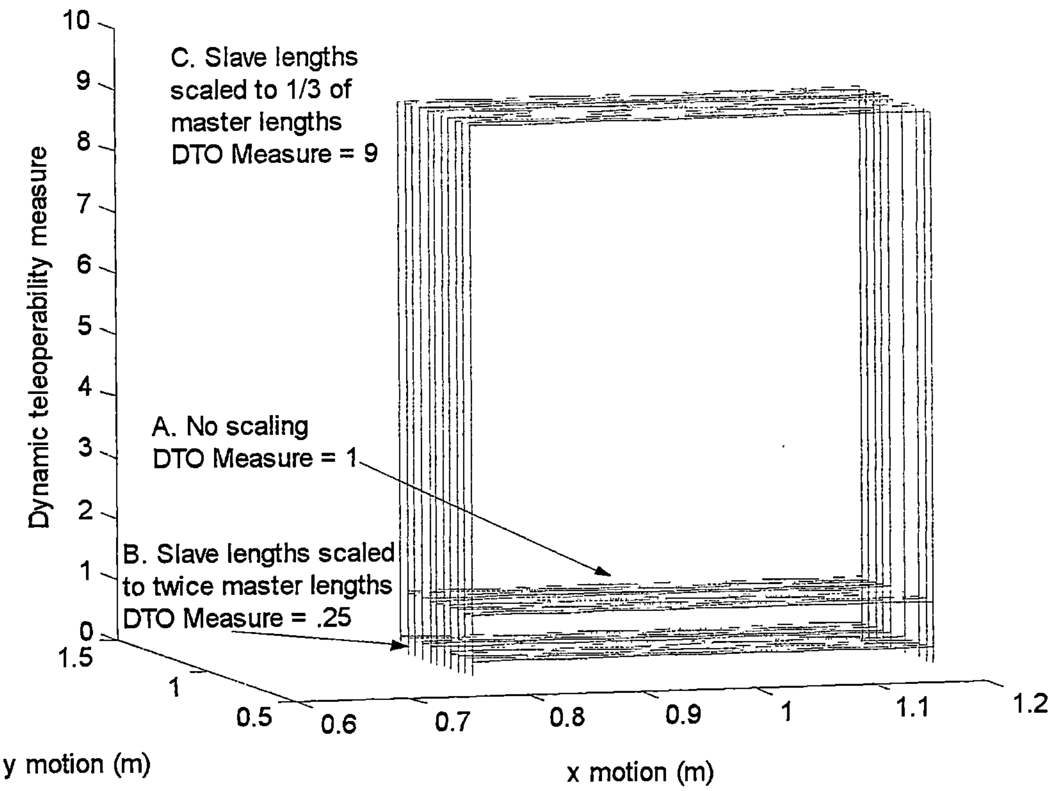

Figure 5.8: Dynamic teleoperability measure in the slave task space from length scaling the slave. The vertical lines are for placement only and do not show the measure going to zero at the edges of the workspaces.

First, consider the slave task space square associated with the no scaling case. The dynamic teleoperability theory asserts that the dynamic teleoperability measure should be 1.0 throughout slave workspace. It is, as shown by case A in Figure 5.8. Since no indexing occurred, the slave workspace is the same as the master workspace of $0.8 \leq x \leq 1.2$, $0.8 \leq y \leq 1.2$ for all three scenarios. As predicted by the dynamic teleoperability theory, when the slave lengths are scaled by a factor β, the dynamic teleoperability measure will be $\frac{1}{\beta^m}$ where m is the size of the end-effector velocity vector as described in section 4.3. For the 2-DOF planar manipulator, the size of the end-effector velocity vector is 2, and the measure agrees and is calculated to be $\frac{1}{\beta^2}$ as shown in cases A, B, and C.

5.2.3 Mass Scaling

The dynamic teleoperability measure for the system was evaluated for three different mass scaling scenarios.

A) No mass scaling between the master and slave (scaling factor $\gamma = 1$)

B) The slave masses scaled to twice the master masses (scaling factor $\gamma = 2$)

C) The slave masses scaled to 1/3 the master masses (scaling factor $\gamma = 1/3$)

Figure 5.9 is a three-dimensional plot of these scenarios. The (x,y) plane is the slave task space plane, and the z-axis is the dynamic teleoperability measure for each point in the slave task space.

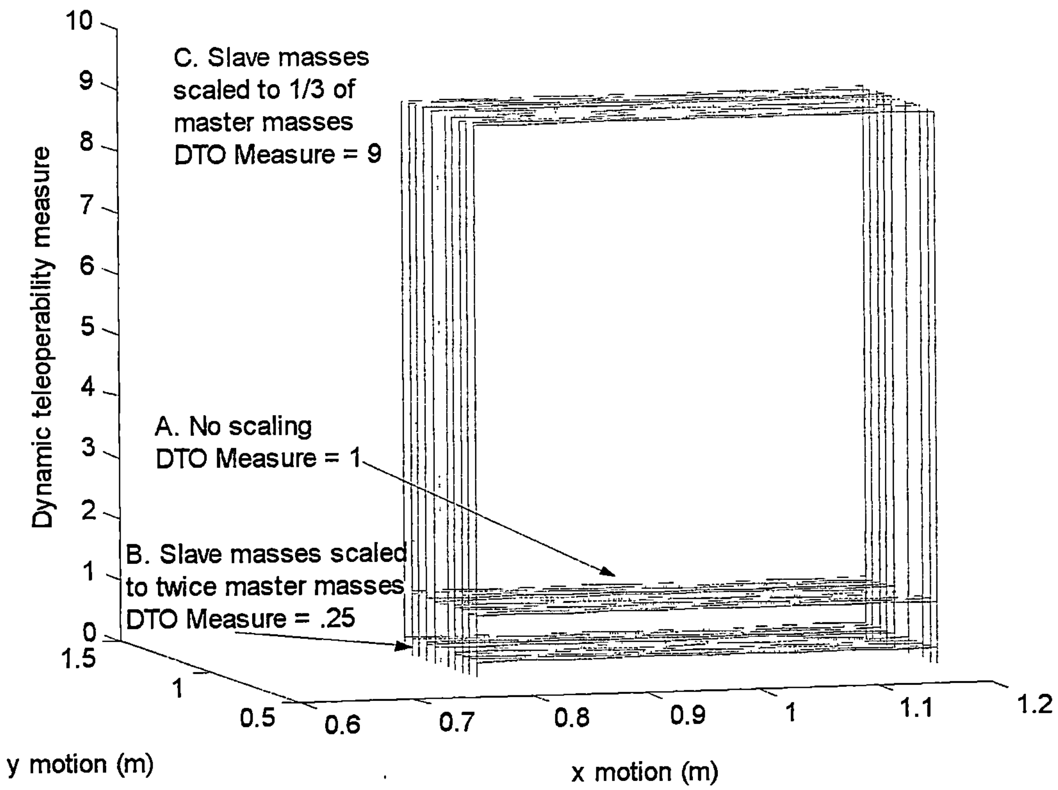

Figure 5.9: Dynamic teleoperability measure in the slave task space from mass scaling the slave. The vertical lines are for placement only and do not show the measure going to zero at the edges of the workspaces.

First, consider the slave task space square associated with the no scaling case. The dynamic teleoperability theory asserts that the dynamic teleoperability measure should be 1.0 throughout slave workspace. It is, as shown by case A in Figure 5.9. Since no indexing occurred, the slave workspace is the same as the master workspace of $0.8 \le x \le 1.2$, $0.8 \le y \le 1.2$ for all three scenarios. As predicted by the dynamic teleoperability theory, when the slave masses are scaled by a factor γ, the dynamic teleoperability measure will be $\frac{1}{\gamma^m}$ where m is the size of the end-effector velocity vector as described in section 4.5. For the 2-DOF planar manipulator, the size of the end-effector velocity vector is 2, and the measure agrees and is calculated to be $\frac{1}{\gamma^2}$ as shown in cases A, B, and C.

6 Experimentation

Experiments were conducted to validate the presented teleoperability and dynamic teleoperability theory results. The experiments were conducted to test one factor affecting the teleoperability and dynamic teleoperability measure, indexing. The experiments were based on a Fitts' test and used the Schilling Titan II manipulator and mini-master.

6.1 Fitts' Test

The Fitts' test was developed in 1954 as a method of modeling human psychomotor behavior **[Mackenzie, 92]**. The relationship between movement time and distance and accuracy results from the "motors" that are used to move a limb. Each movement requires "motor units" that produce forces. Noise is associated with each force due to variations in force duration and amplitude. Noise increases with increased movements, and therefore accuracy decreases **[Draper, 99]**. Fitts presented an index of difficulty based on these variables and given by the equations

$$MT = a + b \cdot ID \tag{6.1}$$

and

$$ID = \log_2\left(\frac{2d}{w}\right) \tag{6.2}$$

where

MT = time to complete movement

a, b = empirically derived constants for human linkages involved

ID = index of difficulty

and

d = movement distance

w = target diameter.

6.2 Setup

The experimental setup consisted of a Schilling Titan II manipulator arm, a Schilling mini-master, the unilateral slave controller, and a modified Fitts' board. The Schilling Titan II is a six-degree-of-freedom hydraulic manipulator constructed primarily of titanium and weighing 225 pounds. It has a reach of approximately 76 inches and a payload capacity at full extension of 240 pounds and when retracted of 1000 pounds. The end-effector is a two-finger gripper with a maximum opening of five inches. It is securely mounted on the lab floor. The manipulator in the Robotics and Electromechanical Systems Laboratory is on loan from Oak Ridge National Laboratory (ORNL) and was a part of the Dual Arm Work Platform (DAWP) **[Hamel, 01]**. Characteristics of the manipulator joints are given in Table 6.1 **[Schilling, 01].**

The unilateral slave controller connects the Titan II to the master arm and is a unilateral 8088 backup control. It may be connected directly to the master controller and slave manipulator to provide joint-to-joint control between the two. Its use requires a master control PROM. From the mini-master, controls are sent to the control computer and then to the slave through the C30 box via a VME bus.

Table 6.1: Schilling Titan II manipulator characteristics.

Joint	Range of Motion	Actuator
azimuth	270°	rotary
shoulder pitch	120°	linear
elbow pitch	270°	rotary
wrist pitch	180°	rotary
wrist yaw	180°	rotary
wrist rotate	360°	gear rotor
gripper	5 inches.	linear

The master arm is a six degree-of-freedom articulated arm with an approximately eleven-inch reach. The box on which it is mounted has a power switch and twelve function keys, an LCD screen, and an RS-232 port with which to communicate with the unilateral slave controller. Control is by a programmable ROM (PROM) which must be installed on the computer board inside the master enclosure. The master arm has a freeze button on its terminal end and two textured bands which may be squeezed to open and close the gripper. In the used unilateral slave control mode, the master screen has a series of menus to determine system parameters such as toggling the hydraulic solenoid to enable the arm hydraulic power.

One subset of the experiments utilized a black and white video camera with the image projected on a nine-inch TV screen. The TV was four inches above the thirty-inch high table on which the mini-master was also placed. The camera was positioned 96 inches to the right of and 60 inches back from the base of the manipulator. The location approximated a forty-five degree camera angle from the plane of the manipulator and modified Fitts' board.

The experimental setup was configured as shown in Figure 6.1 so that the 6 DOF Schilling manipulator could be used in a 3 DOF planar configuration. The modified Fitts' board was placed in the plane of the arm. The planar configuration in which the manipulator was placed allows the experimental results to be compared to the theoretical results presented in Chapter 5. In this setup, the lowest target was 29.5 inches from the floor and 60 inches from the base of the manipulator.

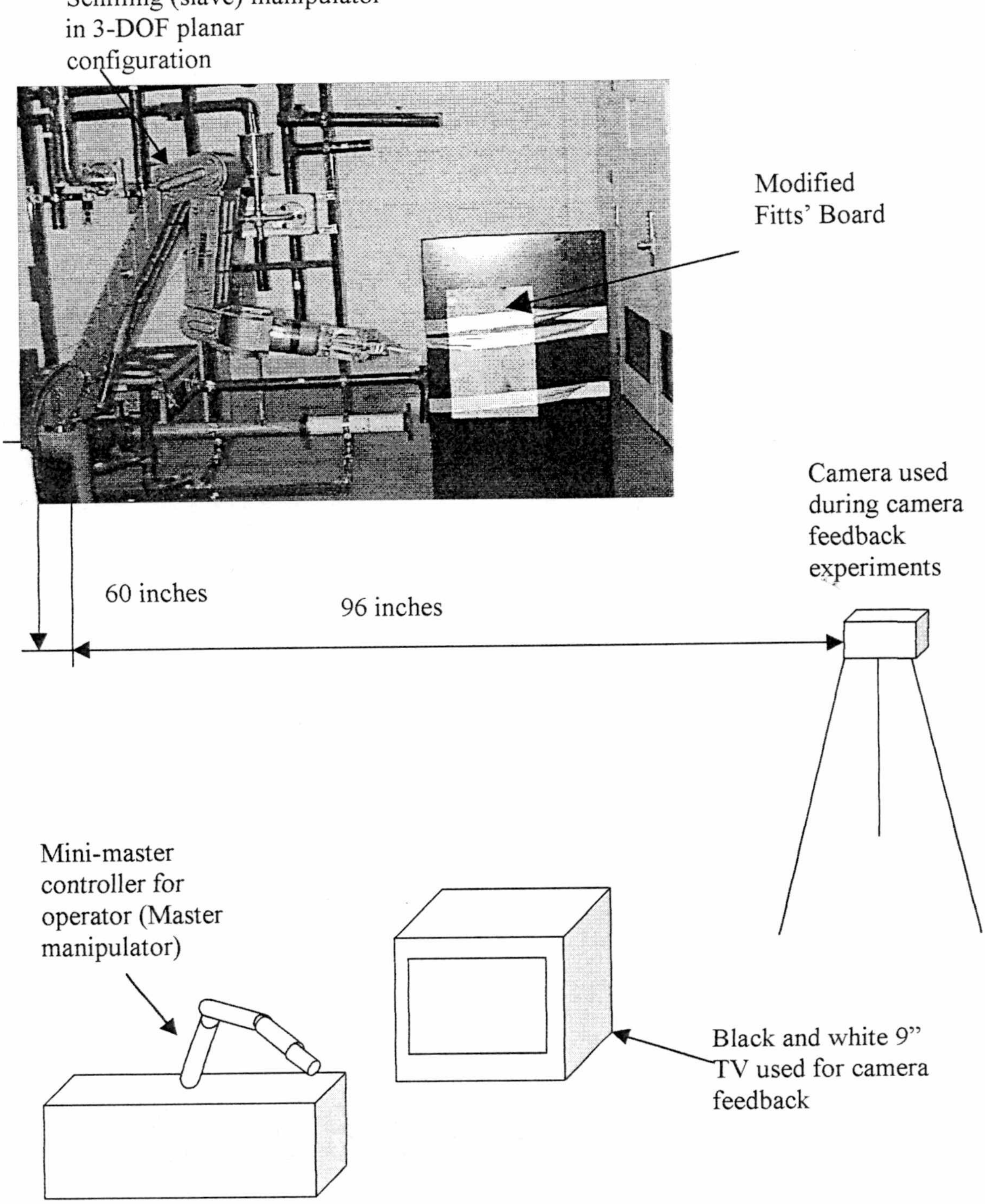

Figure 6.1: Experimental setup including Titan II manipulator and modified Fitts' board.

The modified Fitts' board was constructed as shown in Figure 6.2. The board was constructed of plywood. The targets were approximately half-inch thick circular wooden disks that were drilled through to allow insertion of a screw through the center which was then inserted into holes drilled in the plywood board. The board was attached to the table with duct tape. The duct tape provided secure support for the board. It also provided an elastic coupling to the table. The taping would flex and rebound when hit by the manipulator.

6.3 Initial Experiments

The first experiments used the modified Fitts' board in a 1-D Fitts' reciprocal tapping test. The board was placed horizontally on a table and only two of the three targets were used. This experiment was rejected because it forced the manipulator out of a planar configuration because it had to move vertically and horizontally to touch the targets. In this experiment, indexing was accomplished by rotating the base joint of the mini-master forty-five degrees clockwise and rotating the second and third joints clockwise by approximately ten degrees. This indexing was ineffective because the operator could easily compensate for the rotation and therefore times for indexed cases were as low as for the aligned case. Similar results were found for indexing the second joint by ninety degrees and the first and second joints by forty-five degrees.

Next, the modified Fitts' board was used in a 2-D test. This caused two primary problems. First, the motion could no longer be compared to the planar theory presented. Second, the modified Fitts' board's placement on the table would cause operator error

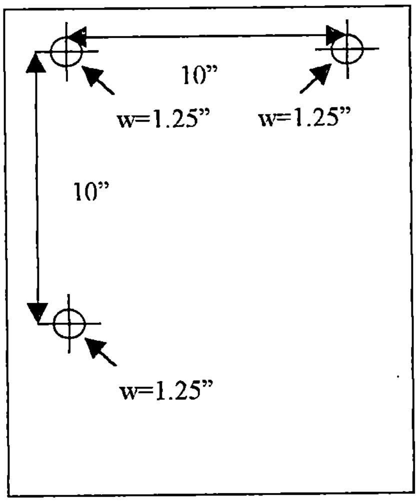

Figure 6.2: Modified Fitts' board.

to result in the manipulator being slammed into the inflexible table. This could have resulted in serious damage to the table or manipulator. In this configuration, an indexing of the base joint by 180 degrees was tested. As the theory predicts, this indexing did not result in any change in task time. The problems discovered during these initial experiments led to the development of the planar Fitts' reciprocal tapping test presented here.

6.4 Method

6.4.1 Operators

Three operators were used for the Fitts' experiments. All three operators are graduate students in the Robotics and Electromechanical Systems Laboratory. Two operators (Operator 1 and 2 in the experiments) had no previous experience with teleoperation of the Titan II although Operator 1 is familiar with both video games and model airplanes. Operator 2 is left-handed. The mini-master must be controlled with the right hand, so the lack of dexterity is an issue for Operator 2. Operator 3 has significant experience in teleoperation of the Titan II. None of the operators had experience using an indexed mini-master.

6.4.2 Procedure

The test was based on the Fitts' reciprocal tapping test. This task typically involves moving between and tapping two targets on a task board. It is representative of object acquisition that occurs in actual teleoperation. In order to increase the task difficulty, a third target was positioned to form a right angle. The targets were touched with a pencil gripped in and taped to the manipulator end-effector. A pencil was used because of its flexing properties. Also, under load, the pencil would break before the board or end-effector could be damaged. Duct tape was used to secure the pencil, so that if the pencil broke, it would remain attached to the manipulator so the test could be completed.

For each test, the time required to complete five circuits was recorded. One circuit consisted of touching the top right, top left, bottom, top left, and top right targets in order as seen from the operator's viewpoint. An ID of 4 was used as the 1.25 inch diameter targets were spaced 10 inches apart. Since the board was in the plane of the manipulator, this test required both vertical movement and the extension of the arm. Touching the target consisted of touching the end of the pencil to the target.

The operators first performed three tests with the mini-master aligned with the manipulator. Then, three additional tests were performed with the second joint of the mini-master indexed 225 degrees as shown in Figure 6.3. This indexing caused motions of the mini-master directed toward the operator to move the manipulator away from the operator. In addition, vertical motions by the operator resulted in the opposing vertical motions by the manipulator. For this set of tests, the operator was controlling the arm through direct visual feedback.

Finally, a second set of experiments was conducted using visual feedback from the camera. The camera location provided some depth perception and maximizes the visibility of the arm in the camera frame. Each of the three operators then performed one

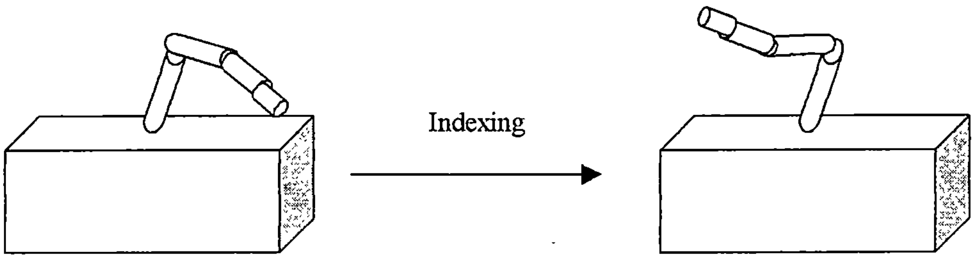

Figure 6.3: Mini-master in experimental non-indexed (left) and indexed (right) configurations. In the non-indexed configuration, the mini-master is in the same configuration as the Titan II slave. In the indexed case, the second joint of the mini-master has been indexed 225 degrees from the configuration of the slave.

additional test with the mini-master aligned and indexed. Use of the camera more realistically simulates typical remote maintenance work.

6.5 Results

Figure 6.4 shows the results of the experiments. For each experimental run, the time for completion of five circuits is presented. The indexing case studied experimentally was intentionally chosen to seriously hinder operator performance. This choice allowed the performance differences to be more noticeable. The results should be "bad" to illustrate the correlation between the teleoperability measure and performance in this case. The following conclusions refer to this indexing configuration, and general conclusions as to the effects of indexing on operator performance should not be drawn from these results. In true teleoperation situations, indexing is only used to increase operator comfort and performance. This figure shows that indexing the second joint of the master by 225 degrees always increased the operator's time. The non-indexed cases show little learning curve and little difference among operators' times. In contrast, the indexed cases show a wide range of times among the operators. The learning curve, or decreasing time in subsequent experimental runs, demonstrates that the operator can learn to significantly compensate for the indexing but Operators 2 and 3 have already leveled off on their times. Even after learning, the completion time is longer than non-indexed as predicted by theory. The teleoperability measure and dynamic teleoperability measures for the specific cases used in this experiment are shown in Figures 6.5 and 6.6 respectively. The deviation from the ideal measure of one predicts decreased performance, and this performance degradation was confirmed by the experimentation.

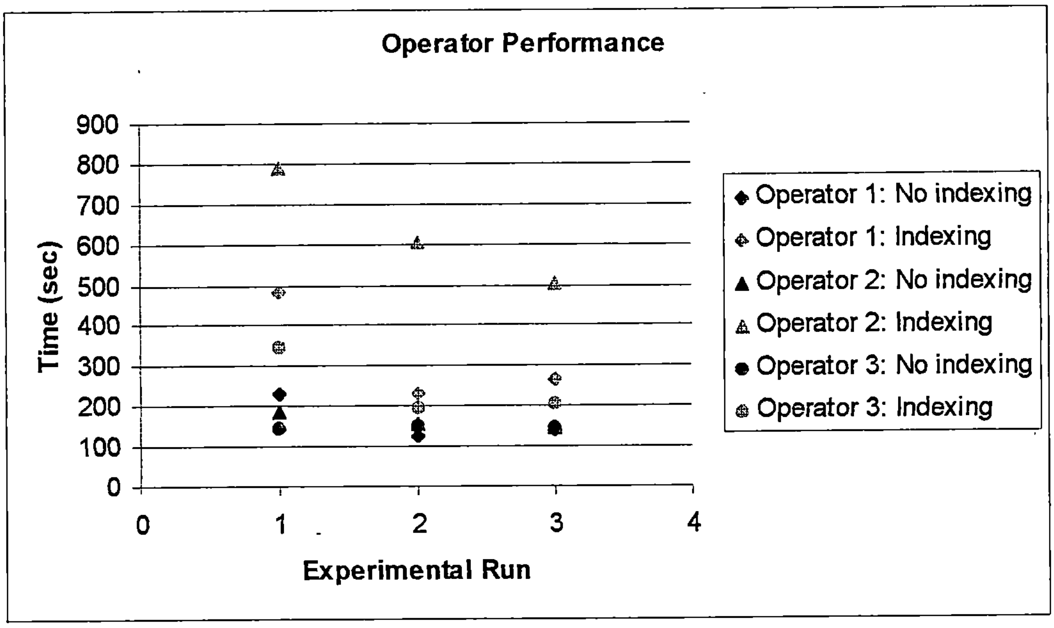

Figure 6.4: Operation time with and without indexing for experimental cases.

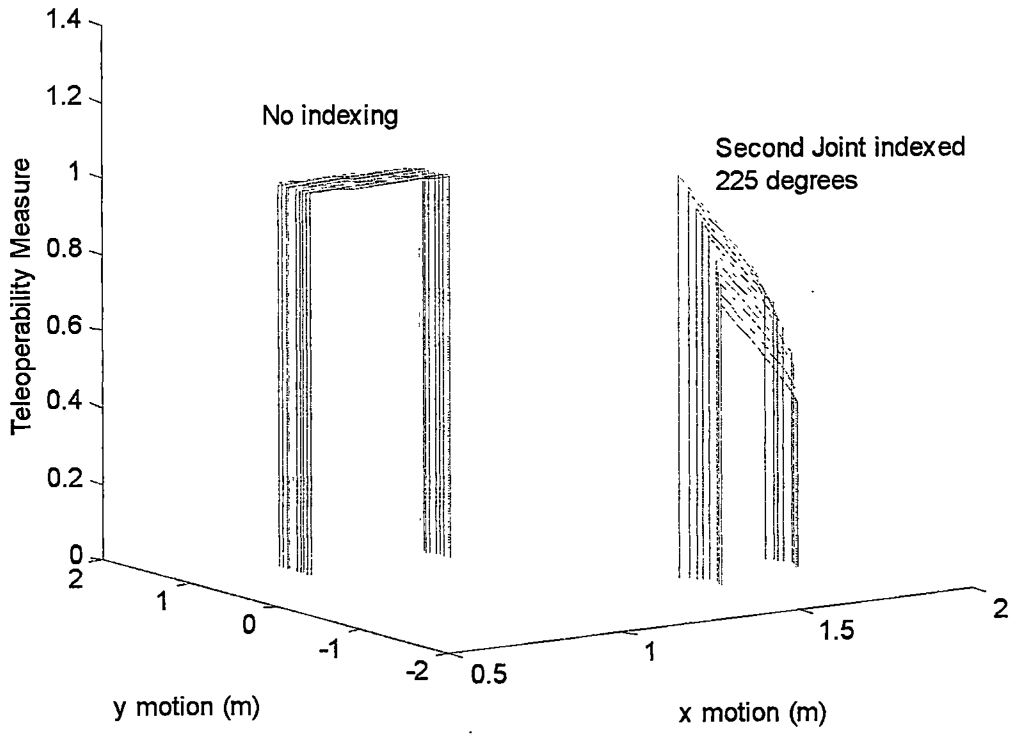

Fig 6.5: Teleoperability measure for experimental cases.

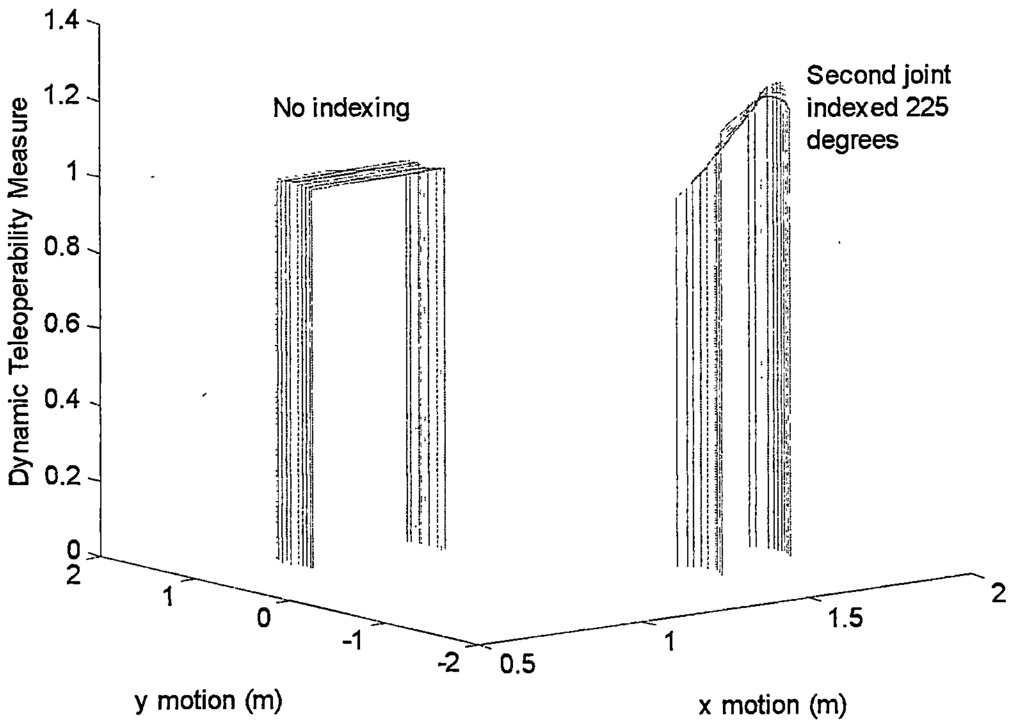

Figure 6.6: Dynamic teleoperability measure for experimental cases.

Table 6.2 presents the average data from the direct viewing experiments and additional data from the experiments conducted with visual feedback from a camera view. It can be seen that in the case of no indexing, the camera has little effect on completion times for two-thirds of the operators. However, all operators' times increased when using the camera in the indexed case. Massimino reports that the primary contribution to cameras increasing performance time is the subtended visual angle **[Massimino, 94].** The camera angle used limited the view. When the manipulator behaved intuitively, the view of the end-effector was sufficient. However, when the manipulator behaved counter-intuitively with the indexing case, a larger viewing area or multiple views are required. Multiple views would provide the operator a truer sense of the overall manipulator motions. It is difficult to draw broad conclusions from the small data set collected. However, this data can be used to observe trends in performance for the specific case tested.

These experiments are for a simple planar configuration. However, they illustrate how these measures might be used. The teleoperability measure is a quantifiable assessment of the "distance" from alignment between the master and the slave. The conjecture is that the greater the "distance" resulting from indexing then the greater the impact on performance. Indirect viewing through video cameras would exacerbate this impact on performance. The simple planar experiments show a direct correlation between the quantifiable distance from alignment (teleoperability measure) and the performance degradation.

Table 6.2: Direct viewing run times (sec) compared to camera feedback times.

	Operator 1 Times	Operator 2 Times	Operator 3 Times
Direct view No indexing	166.33 (avg)	162 (avg)	146 (avg)
Direct view Indexing	327 (avg)	631.66 (avg)	248.66(avg)
Camera feedback No indexing	160	276	148
Camera feedback Indexing	364	Could not complete in 900 sec (15 min)	505

7 Discussion

From the teleoperability and dynamic teleoperability theories, ellipsoids, measures, and simple example cases presented, the following observations can be made about teleoperators and teleoperator design.

For dexterous teleoperator design a similar master with no scaling and a joint-to-joint control system is a simple and robust design. If a dissimilar master is desired such as in a teleoperated system with a redundant slave manipulator, then a Cartesian-based control system or a hybrid controller system with Cartesian positioning and joint-to-joint orientation control is preferred from a teleoperability viewpoint over a joint-to-joint control system with an alternative redundancy resolution. Extending the results of the simple length scaling cases presented to higher DOF systems suggests that if a scaled replica master is desired because of the large size of the slave (e.g., the MLDUA from the Gunite tanks program at ORNL **[Rule, 98]**) or because of space limitations at the master location (e.g., the Spar arm in the space shuttle) then length scaling should be uniform. One may even need to scale the angular velocity commands if preservation of performance fidelity is more important than the actual angular motions.

From experience, it has been shown that indexing in a teleoperated system is a helpful option to increase efficiency and reduce fatigue. If indexing is implemented, then teleoperability and dynamic teleoperability theory guides one to do the following. Indexing the base only is often very helpful and has no effect from a teleoperability or dynamic teleoperability viewpoint. Indexing other joints will change the teleoperability and dynamic teleoperabilty measures and the shape of the teleoperability and dynamic teleoperability ellipsoids. In practice, this has been found to be acceptable as long as the control system is designed with a feature that allows the operator to return the master and slave to an aligned configuration.

The presented results suggest that caution should be used when scaling master to slave commands non-uniformly. As long as scaling is uniform, the size of the slave-space sphere is unaffected. The experimental results from the indexing case suggest that measure uniformity is the critical component of the measure instead of its raw value. Therefore, carefully observe the teleoperability and dynamic teleoperability measures throughout the entire workspace. Slow-moving slave manipulators such as the Spar arm on the space shuttle or the MLDUA on the Gunite tanks should use simple joystick velocity controllers. For these types of master controllers, a "unit velocity sphere" in the master space maps to a "unit velocity sphere" in the slave space and experience suggests that the ability to dexterously manipulate objects is not an issue because of the slow speed (i.e., low bandwidth) of the slave manipulators. It is seen in practice that this is the type of controller selected for these teleoperators.

Teleoperability and dynamic teleoperability can be used in the selection of a teleoperated system. Simplified simulations have been performed that allow manipulator configurations to be chosen for a given workspace. Two workspaces have been studied, a square and an annular region within the square. Two master/slave systems were studied.

The master in both systems was a two link Cartesian manipulator. The slaves were a two link theta-theta and an r-theta manipulator. In both workspaces, the theta-theta manipulator was deemed optimal. It had a lower standard deviation of both the teleoperability and dynamic teleoperability measures. The size of the annular region was then increased and decreased, and the same conclusion remained.

Because the teleoperability measure is a maximum whenever the master and slave are perfectly aligned, it could be used in a bilateral controller. Figure 7.1 illustrates a schematic controller that uses the teleoperability measure to modify the traditional force-reflecting commands passing between the master and slave. In the figure, F_H represents the hand force from the human operator, and F_{ENV} represents the force from the environment at the slave end. The subscripts M and S refer to Master and Slave respectively. The vector of joint angles is $\mathbf{q}$ and $\mathbf{J}^T$ is the Jacobian transpose. The controller and dynamics block represent the "normal" joint control laws (e.g., simple PD controller) and the arm dynamics. The optimization routine could be any multi-dimensional optimization scheme that would be able to maximize the teleoperability measure over the joint angle space. The set of joint angle changes for both the master ($\Delta\mathbf{q}_M$) and the slave ($\Delta\mathbf{q}_S$) would be used to modify the traditional command error of the respective angular differences. The joint angle differences would distribute throughout the master and slave arms because the external forces (hand or environment) are not uniformly distributed throughout the entire arm. Adding the teleoperability-based modified signal would tend to align the slave to the master and adjust for this non-uniform distribution.

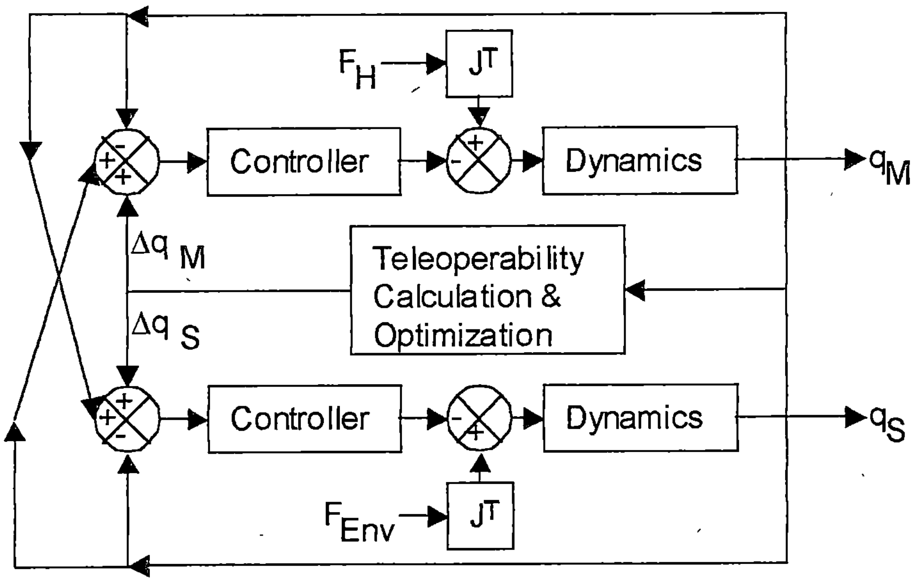

Figure 7.1: Controller schematic using the teleoperability measure to modify the traditional force-reflecting commands.

Another simulation was performed using the Cartesian master and both the theta-theta and r-theta slaves. For each master/slave set, the standard deviation of the dynamic teleoperability measure was studied over the same workspace. The workspace was the first quadrant, between zero and ninety degrees. In this quadrant, narrow arc segments beginning at a fixed radius (rmin) and covering a change in radius of 0.1 were studied throughout the workspace of the slave. Results of this simulation are shown in Figure 7.2. These results are for the system configuration that locates the link masses at the center of the links. The results show that in the middle of the workspace, both slaves perform similarly from a dynamic teleoperability viewpoint. However, as the slave nears the kinematic singularity at the edge of the workspace at 2, the r-theta slave standard deviation continues to decrease while the theta-theta standard deviation starts to increase exponentially. In this simulation, the transition occurs at approximately 1.75. These results suggest that if the task is to be conducted near the edge of the workspace, the r-theta slave should be chosen. If the theta-theta is needed then the task location should be moved. These results are due to the increased movement of the link masses that the theta-theta slave must produce near the edge of the workspace that are not required by the more static r-theta slave that "sees" the same mass movement at any location in the workspace. This simulation was then repeated with the link masses located at 0.1, 0.25, 0.4, and 0.75 the link lengths. The trends of the standard deviation of the dynamic teleoperability measures were similar for these cases. When the masses are close to the base of the link, the r-theta is always better. As the masses move past center (LC = 0.5L) and toward the end of the links, the transition point moves out as well to a location of 1.9 when the masses are at 0.75 the link lengths.

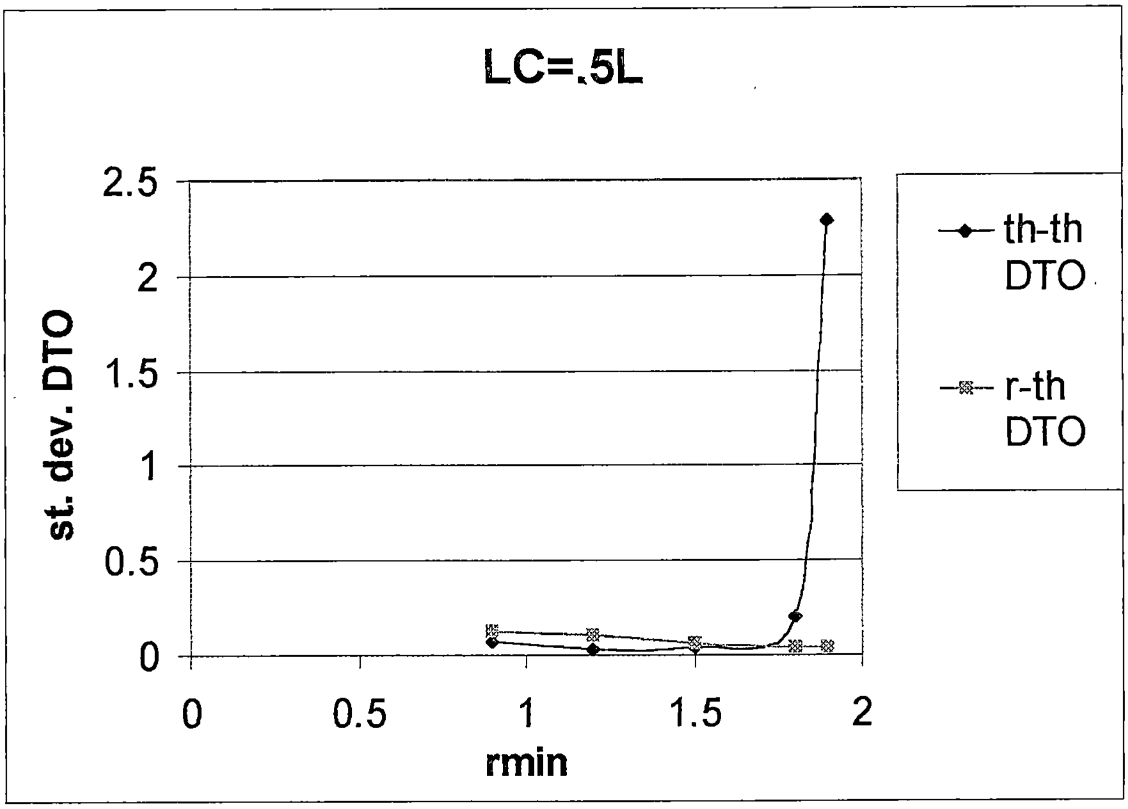

Figure 7.2: Standard deviation of dynamic teleoperability measure for Cartesian master and theta-theta and r-theta slave simulations.

This thesis has presented the foundational theory of teleoperability and dynamic teleoperability and examined the teleoperability and dynamic teleoperability measures for simple, representative cases. Additional work will include the exploration of alternative teleoperability and dynamic teleoperability measures that address some of the assumptions made during the presented theoretical development. These new measures can then be tested in 2-DOF, 3-DOF, and theta-theta versus r-theta simulations as was done in this thesis. Additionally, new measures could be developed that reveal new insight into the teleoperated system. Paralleling Yoshikawa's developments of alternative manipulability measures, the ratio of minimum to maximum singular values should be studied as an index of directional uniformity of the ellipsoids. Also, the minimum singular value should be studied as a possible measure that will give the minimum teleoperation or dynamic teleoperation ability of a system. In the future, more detailed simulations and experiments should be performed on higher DOF systems that more accurately reflect the types of manipulator systems used in teleoperation. Different types of manipulators could be studied experimentally and the r-theta and theta-theta simulation could be validated experimentally. In addition, a simulation could be performed on the ASM from ORNL. This simulation would allow joint failure data to be studied. New experiments could extend the Fitts' reciprocal tapping test to an assembly experiment. This experiment would allow the evaluation of the teleoperability and dynamic teleoperability measures in a task that is closer to true remote work. Additional experiments could also be used to analyze position-force controlled teleoperator systems as described in section 4.11.

8 Conclusions

The concepts of manipulability and dynamic manipulability can be used to evaluate a robotic manipulator. This thesis expands these topics to the concepts of teleoperability and dynamic teleoperability which can be used to evaluate teleoperated master/slave manipulator systems. The mathematical developments of teleoperability and dynamic teleoperability have been presented. The behavior of the teleoperability and dynamic teleoperability measures in various operational conditions has been presented for 2 and 3 DOF systems. Special attention was given to the effects of indexing, length scaling, and mass scaling between the master and slave. Simple experimental results have validated the theory. Teleoperability, dynamic teleoperability and the associated teleoperability and dynamic teleoperability ellipsoids and measures should be useful concepts in design, implementation, and selection of teleoperated systems. Specifically, this theory may be useful in the selection of master and slave configurations, guide in control system design, and provide insight into necessary and/or helpful operational features for teleoperated and telerobotic systems. Future work will include additional measures that accommodate assumptions made in this development and measures that explore other aspects of teleoperability and dynamic teleoperability. In the future, simulations and experiments will also be conducted that more closely resemble realistic teleoperation with higher DOF manipulator systems performing more complex tasks.

REFERENCES

[Chiacchio, 92] P. Chiacchio, S. Chiaverini, L. Sciavicco, and B. Siciliano, "Influence of Gravity on the Manipulability Ellipsoid for Robot Arms," *ASME J. Dynamic Systems, Measurement, and Control*, vol. 114, pp. 723-727, 1992.

[Craig, 89] J. J. Craig, *Introduction to Robotics*. Reading, MA: Addison-Wesley, 1989.

[Draper, 99] J. V. Draper, B. C. Jared, and M. Noakes, "Manipulator Performance Evaluation Using Fitts' Tapping Test," in Proceedings of *The Eighth ANS Topical Meeting on Robotics and Remote Systems*, 1999.

[Goertz, 52] R. C. Goertz, "Fundamentals of General-Purpose Remote Manipulators," *Nucleonics*, vol. 10, no. 11, pp. 36-45, Nov. 1952.

[Goertz, 54] R. C. Goertz, "Electronically Controlled Manipulator," *Nucleonics*, vol. 12, no. 11, pp. 46-47, Nov. 1954.

[Flateau, 65] C. R. Flateau, "Development of Servo Manipulators for High Energy Accelerator Requirements," in *Proceedings of the 13th Conference on Remote Systems Technology*, 1965, pp. 29-35.

[Hamel, 01] W. Hamel, S. Kim, G. Zhang, R. Dubey, and P. Murray, "Human Machine Cooperative Telerobotics Topical Report," for *The Department of Energy*, 2001.

[Johnsen, 67] E. G. Johnsen and W. R. Corliss, "Teleoperators and Human Augmentation," NASA SP-5047, Dec. 1967.

[Kaye, 92] A. Kaye, C. Walker, and P. Pauling, "Hydraulic Position Control of the JET Microwave Antenna," JET Publication, JET-P (92)87, Oct. 1992.

[Klein, 85] C. A. Klein, "Use of Redundancy in the Design of Robotic Systems," in *Robotics Research: The Second International Symposium*, ed. H. Hanafusa and H. Inoue, MIT Press, 1985, pp. 207-214.

[Kress, 97] R. L. Kress, J. F. Jansen, and M. W. Noakes, "The Evolution of Teleoperated Manipulators at ORNL," in *Proceedings of The Seventh ANS Topical Meeting on Robotics and Remote Systems*, 1997, pp. 623-631.

[Maciejewski, 89] A. A. Maciejewski and C. A. Klein, "The Singular Value Decomposition: Computation and Applications to Robotics," *Int. J. of Rob. Res.*, vol. 8, no. 6, pp. 63-79, Dec. 1989.

[MacKenzie, 92] I. S. MacKenzie, "Fitts' Law as a Research and Design Tool in Human-Computer Interaction," *Human-Computer Interaction*, vol. 7, pp. 91-139, 1992.

[Massimino, 94] M. J. Massimino and T. B. Sheridan, "Teleoperator Performance with Varying Force and Visual Feedback," *Human Factors*, vol. 36, no. 1, pp. 145-157, 1994.

[Raimondi, 88] T. Raimondi, "Three Lectures," presented at the Advances in Teleoperation for International Center for Mechanical Sciences, Udine, Italy, 1988.

[Rule, 98] V. A. Rule, B. L. Burks, and S. D. Van Hoesen, "North Tank Farm Data Report for the Gunite and Associated Tanks at Oak Ridge National Laboratory, Oak Ridge, Tennessee," ORNL/TM-13630, May 1998.

[Salisbury, 82] J. K. Salisbury and J. J. Craig, "Articulated Hands, Force Control and Kinematic Issues," *Int. J. of Rob.Res.*, vol. 1, no. 1, pp. 4-17, 1982.

[Sciavicco, 00] L. Sciavicco and B. Siciliano, *Modelling and Control of Robot Manipulators*. London: Springer-Verlag, 2000.

[Schilling, 01] Schilling, "Titan System Specifications," www.schilling.com [Online], October 2001.

[Vertut, 85] J. Vertut and P. Coiffet, *Teleoperation and Robotics: Evolution and Development, Vol. 3A*. London: Hermes Publishing, 1985.

[Yokokohji, 93] Y. Yokokohji and T. Yoshikawa, "Design Guide of Master Arms Considering Operator Dynamics," *J. of Dynamic Systems, Measurement, and Control*, vol. 115, pp. 253-260, June 1993.

[Yoshikawa, 84] T. Yoshikawa, "Analysis and Control of Robot Manipulators with Redundancy," in *Robotics Research: The First International Symposium*, ed. M. Brady and R. Paul, MIT Press, 1984, pp. 735-747.

[Yoshikawa, 85a] T. Yoshikawa, "Manipulability of Robotic Mechanisms," *Int. J. of Rob. Res.*, vol. 4, no. 2, pp. 3-9, 1985.

[Yoshikawa, 85b] T. Yoshikawa, "Dynamic Manipulability of Robot Manipulators," *Journal of Robotic Systems*, vol. 2, no. 1, pp. 113-124, 1985.

[Yoshikawa, 86] T. Yoshikawa, "Analysis and Design of Articulated Robot Arms from the Viewpoint of Dynamic Manipulability," in *Robotics Research: The Third International Symposium*, ed. O. Faugeras and G. Giralt, MIT Press, 1986, pp. 273-279.

[Yoshikawa, 90] T. Yoshikawa, *Foundations of Robotics*. Cambridge, MA: The MIT Press, 1990.

APPENDIX

```
% This file is for the teleoperability calculations.
% Latest Modification: 8/23/01
% The base model is the 3dof planar manipulator presented in example 2.16
% on page 58 of Foundations of Robotics by Yoshikawa. This program will
% calculate the teleoperability measure for different configurations.
%

% Basic Manipulator Parameters for Master and Slave
Master_Scale = 1           % Scale factor Master/Slave
rot1=0                        % slave joint 1 indexing
rot2=0                        % slave joint 2 indexing

lM1 = 1.0*Master_Scale;          % Master length 1
lM2 = 1.0*Master_Scale;          % Master length 2
lM3 = 1.0*Master_Scale;          % Master length 3

lS1 = 1.0;                    % Slave length 1
lS2 = 1.0;                    % Slave length 2
lS3 = 1.0;                    % Slave length 3


% The following loops "move" the master through a region in its workspace
% and the slave will follow however it is set up (i.e. replica, scaled,
% indexed, etc.). The inverse kinematics were taken from my derivations
% and pages 126-128 of Craig.

% Initialize loop parameter

alphaM       = 0.0;           % This is the master orientation (rads)

xMstart    = 0.8*Master_Scale;      % Beginning x value
xMend      = 1.2*Master_Scale;      % Ending x value
xincrements = 10;                % Increments between start and end
xMdelta    = (xMend-xMstart)/xincrements;

yMstart    = 0.8*Master_Scale;      % Beginning y value
yMend      = 1.2*Master_Scale;      % Ending y value
yincrements = 10;                % Increments between start and end
yMdelta    = (yMend-yMstart)/yincrements;


% Run through the x Master and y Master loops

for ixM = 0:1:xincrements,                    % Master x loop
    xM = xMstart + ixM*xMdelta;                  % Master x position
```

```
for iyM = 0:1:yincrements,                % Master y loop
    yM = yMstart + iyM*yMdelta;               % Master y position

% Do the inverse kinematics on (xM, yM, alpha)

    xMprime  = xM - lM3*cos(alphaM);           % Intermediate variable
    yMprime  = yM - lM3*sin(alphaM);       % Intermediate variable

    num      = xMprime^2 + yMprime^2 - lM1^2 - lM2^2;
    den      = 2.0*lM1*lM2;
    thetaM(2) = acos(num/den);           % Master angle 2 (between 0 & pi)

    beta     = atan2(yMprime,xMprime);     % Intermediate variable

    num      = xMprime^2 + yMprime^2 + lM1^2 - lM2^2;
    den      = 2.0*lM1*sqrt(xMprime^2 + yMprime^2);
    psi      = acos(num/den);              % Intermediate variable
    thetaM(1) = beta - psi;                    % Master angle 1 (<0)

    thetaM(3) = alphaM - thetaM(1) - thetaM(2);    % Master angle 3


% Set the Slave Angles as Desired

    thetaS(1) = thetaM(1)+rot1;        % Add indexing here if desired
    thetaS(2) = thetaM(2)+rot2;        % Add indexing here if desired
    thetaS(3) = thetaM(3);                 % Add indexing here if desired


% Calculate Master Jacobian

    c1      = cos(thetaM(1));
    c2      = cos(thetaM(2));
    c3      = cos(thetaM(3));
    c12= cos(thetaM(1) + thetaM(2));
    c123    = cos(thetaM(1) + thetaM(2) + thetaM(3));
    s1      = sin(thetaM(1));
    s2      = sin(thetaM(2));
    s3      = sin(thetaM(3));
    s12= sin(thetaM(1) + thetaM(2));
    s123    = sin(thetaM(1) + thetaM(2) + thetaM(3));

    jM11    = -(lM1*s1 + lM2*s12 + lM3*s123);
```

```
jM12  = -(lM2*s12 + lM3*s123);
jM13  = -(lM3*s123);

jM21  = (lM1*c1 + lM2*c12 + lM3*c123);
jM22  = (lM2*c12 + lM3*c123);
jM23  = (lM3*c123);

jM31  = 1;
jM32  = 1;
jM33  = 1;

jM    = [jM11,jM12,jM13;
         jM21,jM22,jM23;
         jM31,jM32,jM33];


% Calculate Slave Jacobian

c1    = cos(thetaS(1));
c2    = cos(thetaS(2));
c3    = cos(thetaS(3));
c12= cos(thetaS(1) + thetaS(2));
c123  = cos(thetaS(1) + thetaS(2) + thetaS(3));
s1    = sin(thetaS(1));
s2    = sin(thetaS(2));
s3    = sin(thetaS(3));
s12   = sin(thetaS(1) + thetaS(2));
s123  = sin(thetaS(1) + thetaS(2) + thetaS(3));

jS11  = -(lS1*s1 + lS2*s12 + lS3*s123);
jS12  = -(lS2*s12 + lS3*s123);
jS13  = -(lS3*s123);

jS21  = (lS1*c1 + lS2*c12 + lS3*c123);
jS22  = (lS2*c12 + lS3*c123);
jS23  = (lS3*c123);

jS31  = 1;
jS32  = 1;
jS33  = 1;

jS    = [jS11,jS12,jS13;
         jS21,jS22,jS23;
         jS31,jS32,jS33];
```

```
% Calculate the slave position to be used in data display

        xS      = lS1*c1 + lS2*c12 + lS3*c123;  % Current slave x position
        yS      = lS1*s1 + lS2*s12 + lS3*s123;  % Current slave y position

% Calculate Teleoperation Jacobian and Transpose

        jSi     = inv(jS);
    jMp         = pinv(jM);
    jTO         = jS*jMp;
        jTOT    = jTO';
%temp=jTO*jTOT

% Calculate the Teleoperability Measure

        TO_Measure = sqrt(det(jTO*jTOT));

% Set up the 3D plot

        if ixM == 0                     % Store base point for making plot pretty
            X(1,iyM+1) = xS;
            Y(1,iyM+1) = yS;
            Z(1,iyM+1) = 0.0;
        elseif ixM == xincrements       % Store base point for making plot pretty
            X(xincrements+3,iyM+1) = xS;
            Y(xincrements+3,iyM+1) = yS;
            Z(xincrements+3,iyM+1) = 0.0;
        end

        X(ixM+2,iyM+1) = xS;
        Y(ixM+2,iyM+1) = yS;
        Z(ixM+2,iyM+1) = TO_Measure;


    end                         % end of y loop for the master
end                             % end of x loop for the master


% 3D Plotting section

plot3(X,Y,Z);
```

```
% This file is for  dynamic teleoperability calculations.
% Pamela Murray Latest Modification: 10/22/01
%The manips are 2dof planars  presented on p. 150 of Sciavicco


%Scaling
Master_Scale = 1;      % length Scale factor Master/Slave
Slave_Scale = 1;       % length Scale factor Slave/Slave
rot1=0;                    % for thetaS(1) = thetaM(1)+rot1;
rot2=0;                % for thetaS(2) = thetaM(2)+rot2;
Master_mass_scale1=1;  % for mM1=1*Master_mass_scale1; (scaled) mass of Master
link 1
Master_mass_scale2=1;  % for mM2=1*Master_mass_scale2; (scaled) mass of Master
link 2
Slave_mass_scale1=1/3; % for mS1=1*Slave_mass_scale1; (scaled) mass of Slave link
1
Slave_mass_scale2=1/3; % for mS2=1*Slave_mass_scale2; (scaled) mass of Slave link
2


%Master (Planar)

lM1 = 1.0*Master_Scale;        % Master length 1
lM2 = 1.0*Master_Scale;        % Master length 2
lcM1=.5*lM1;          %distance of the center of mass of Master link 1
lcM2=.5*lM2;          %distance of the center of mass of Master link 2
mM1=1*Master_mass_scale1 ;          %mass of Master link 1
mM2=1*Master_mass_scale2 ;          %mass of Master link 2
mrM1=0;          %mass of rotor of Master motor 1
mrM2=0;          %mass of rotor of Master motor 2
iM1=0 ;          %moment of inertia relative to center of mass of Master link 1
iM2=0 ;          %moment of inertia relative to center of mass of Master link 2
irM1=0;          %moment of inertia wrt the axes of Master rotor 1
irM2=0;          %moment of inertia wrt the axes of Master rotor 2
krM1=1;          %gear reduction ratio of Master motor 1
krM2=1;          %gear reduction ratio of Master motor 2

%Slave parameters
lS1 = 1.0*Slave_Scale;         % Slave length 1
lS2 = 1.0*Slave_Scale;         % Slave length 2
lcS1=.5*lS1;          %distance of the center of Sass of Slave link 1
lcS2=.5*lS2;          %distance of the center of mass of Slave link 2
mS1=1*Slave_mass_scale1;          %(scaled) mass of Slave link 1
mS2=1*Slave_mass_scale2 ;         %(scaled) mass of Slave link 2
```

```
mrS1=0;          %mass of rotor of Slave motor 1
mrS2=0;          %mass of rotor of Slave motor 2
iS1=0 ;          %moment of inertia relative to center of mass of Slave link 1
iS2=0 ;          %moment of inertia relative to center of mass of Slave link 2
irS1=0;          %moment of inertia wrt the axes of Slave rotor 1
irS2=0;          %moment of inertia wrt the axes of Slave rotor 2
krS1=1;          %gear reduction ratio of Slave motor 1
krS2=1;          %gear reduction ratio of Slave motor 2

% The following loops "move" the master through a region in its workspace
% and the slave will follow however it is set up (i.e. replica, scaled,
% indexed, etc.). The inverse kinematics were taken from my derivations
% and pages 126-128 of Craig.

% Initialize loop parameter
alphaM       = 0.0;          % This is the master orientation (rads)

xMstart    = 0.8*Master_Scale;      % Beginning x value
xMend      = 1.2*Master_Scale;      % Ending x value
xincrements = 10;                   % Increments between start and end
xMdelta    = (xMend-xMstart)/xincrements;

yMstart    = 0.8*Master_Scale;      % Beginning y value
yMend      = 1.2*Master_Scale;      % Ending y value
yincrements = 10;                   % Increments between start and end
yMdelta    = (yMend-yMstart)/yincrements;


% Run through the x Master and y Master loops
for ixM = 0:1:xincrements,                  % Master x loop
   xM = xMstart + ixM*xMdelta;                 % Master x position

   for iyM = 0:1:yincrements,               % Master y loop
      yM = yMstart + iyM*yMdelta;              % Master y position


% Do the inverse kinematics on (xM, yM)
      a        = xM^2 + yM^2 + lM1^2 + lM2^2;          % Intermediate variable
      b        = (xM^2 + yM^2)^2   + lM1^4 + lM2^4;    % Intermediate variable
   c          = xM^2 + yM^2 + lM1^2 - lM2^2;       % Intermediate variable
      d        = xM^2 + yM^2 - lM1^2 - lM2^2;       % Intermediate variable
   k          = sqrt(a^2-2*b);         % Intermediate variable
      beta   = atan2(yM,xM);          % Intermediate variable
   gamma     = atan2(k,c);            % Intermediate variable
```

```
thetaM(1) = beta - gamma;          % Master angle 1
    thetaM(2) = atan2(k,d);            % Master angle 3


% Calculate Master Jacobian
        c1      = cos(thetaM(1));
        c2      = cos(thetaM(2));
        c12= cos(thetaM(1) + thetaM(2));
  s1      = sin(thetaM(1));
        s2      = sin(thetaM(2));
        s12     = sin(thetaM(1) + thetaM(2));

  jM11   = -(lM1*s1 + lM2*s12);
        jM12   = -(lM2*s12);
        jM21   = (lM1*c1 + lM2*c12);
        jM22   = (lM2*c12);
        jM31   = 0;
        jM32   = 0;

        jM     = [jM11,jM12;
                  jM21,jM22];

%Calculate Master inertia (MM) matrix

MM11=iM1+mM1*lcM1^2+krM1^2*irM1+iM2+mM2*(lM1^2+lcM2^2+2*lM1*lcM2*
c2)+irM2+mrM2*lM1^2;

MM12=iM2+mM2*(lcM2^2+lM1*lcM2*c2)+ krM2*irM2;

MM21=MM12;

MM22=iM2+mM2*lcM2^2+krM2^2*irM2 ;

MM       = [MM11,MM12;
            MM21,MM22];


% Set the Slave Angles as Desired
 %rotation between joints
        thetaS(1) = thetaM(1)+rot1;       % Add indexing here if desired
        thetaS(2) = thetaM(2)+rot2;       % Add indexing here if desired


% Calculate slave Jacobian
```

```
c1      = cos(thetaS(1));
c2      = cos(thetaS(2));
c12= cos(thetaS(1) + thetaS(2));
s1      = sin(thetaS(1));
s2      = sin(thetaS(2));
s12     = sin(thetaS(1) + thetaS(2));

jS11    = -(lS1*s1 + lS2*s12);
jS12    = -(lS2*s12);
jS21    = (lS1*c1 + lS2*c12);
jS22    = (lS2*c12);
jS31    = 0;
jS32    = 0;

jS      = [jS11,jS12;
           jS21,jS22];

%Calculate Slave inertia (SS) matrix

SM11=iS1+mS1*lcS1^2+krS1^2*irS1+iS2+mS2*(lS1^2+lcS2^2+2*lS1*lcS2*c2)+irS2
+mrS2*lS1^2;

SM12=iS2+mS2*(lcS2^2+lS1*lcS2*c2)+ krS2*irS2;

SM21=SM12;

SM22=iS2+mS2*lcS2^2+krS2^2*irS2 ;

SM      = [SM11,SM12;
  SM21,SM22];

% Calculate the slave position to be used in data display

xS      = lS1*c1 + lS2*c12 ;  % Current slave x position
yS      = lS1*s1 + lS2*s12 ;  % Current slave y position


% Calculate Dynamic Teleoperation Jacobian and Transpose

jSp     = pinv(jS);
%MSi    = inv(SM);
MMi     =(inv(MM));
jMp     =pinv(jM);
%jDTO_old       = jS*MSi*MM*jMp;
jDTOp   =jM*MMi*SM*jSp;
```

```
    jDTO       = pinv(jDTOp);
        jDTOT= jDTO';
    %mass_var=MMi*SM
        jac_var=jM*jSp;
    jTO=jS*jMp;
    jTOT=jTO';
% Calculate the Dynamic Teleoperability Measure
temp_check_size=jTO*jTOT;
DTO_Measure = sqrt(det(jDTO*jDTOT));
TO_Measure = sqrt(det(jTO*jTOT));

% Set up the 3D plot

        if ixM == 0                     % Store base point for making plot pretty
            X(1,iyM+1) = xS;
            Y(1,iyM+1) = yS;
            Z(1,iyM+1) = 0.0;
        elseif ixM == xincrements       % Store base point for making plot pretty
            X(xincrements+3,iyM+1) = xS;
            Y(xincrements+3,iyM+1) = yS;
            Z(xincrements+3,iyM+1) = 0.0;
        end

        X(ixM+2,iyM+1) = xS;
        Y(ixM+2,iyM+1) = yS;
        Z(ixM+2,iyM+1) = DTO_Measure;

    end                         % end of y loop for the master
end                             % end of x loop for the master

%Calculate std dev of measure
%for square
Z1=Z(2:12,1);
Z2=Z(2:12,2);
Z3=Z(2:12,3);
Z4=Z(2:12,4);
Z5=Z(2:12,5);
Z6=Z(2:12,6);
Z7=Z(2:12,7);
Z8=Z(2:12,8);
Z9=Z(2:12,9);
Z10=Z(2:12,10);
Z11=Z(2:12,11);
dto_vector=[Z1;Z2;Z3;Z4;Z5;Z6;Z7;Z8;Z9;Z10;Z11];
std(dto_vector)
```

```
% 3D Plotting section

plot3(X,Y,Z);
```

VITA

Pamela Murray was born on April 27, 1978, in Knoxville, Tennessee. She graduated from Karns High School in Knoxville, Tennessee, in 1996 as a valedictorian. During her undergraduate years at The University of Tennessee, she was a Tennessee Scholar and worked at Atom Sciences, Oak Ridge National Laboratory, and Woods Hole Oceanographic Institution. She received the Bachelor's degree in Mechanical Engineering summa cum laude from The University of Tennessee in May 2000. As a Master's student at The University of Tennessee in the Department of Mechanical and Aerospace Engineering and Engineering Science, she was a graduate research assistant in the Robotics and Electromechanical Systems Laboratory. Her thesis research on teleoperability and dynamic teleoperability was conducted under the guidance of Dr. Reid Kress.